HHS Public Access

Author manuscript

Brain Behav Immun. Author manuscript; available in PMC 2024 March 01.

Published in final edited form as:

Brain Behav Immun. 2023 March ; 109: 204–218. doi:10.1016/j.bbi.2023.01.009.

Treadmill workout activates PPARα in the hippocampus to upregulate ADAM10, decrease plaques and improve cognitive functions in 5XFAD mouse model of Alzheimer's disease

Suresh B. Rangasamy[1], **Malabendu Jana**[1], **Sridevi Dasarathi**[2], **Madhuchhanda Kundu**[1], **Kalipada Pahan, Ph.D.**[1,2]

[1]Division of Research and Development, Jesse Brown Veterans Affairs Medical Center, Chicago, USA;

[2]Department of Neurological Sciences, Rush University Medical Center, Chicago, USA

Abstract

Although liver is rich in peroxisome proliferator-activated receptor α (PPARα), recently we have described the presence of PPARα in hippocampus where it is involved in non-amyloidogenic metabolism of amyloid precursor protein (APP) via ADAM10, decreasing amyloid plaques and improving memory and learning. However, mechanisms to upregulate PPARα *in vivo* in the hippocampus are poorly understood. Regular exercise has multiple beneficial effects on human health and here, we describe the importance of regular mild treadmill exercise in upregulating PPARα *in vivo* in the hippocampus of 5XFAD mouse model of Alzheimer's disease. We also demonstrate that treadmill exercise remained unable to stimulate ADAM10, reduce plaque pathology and improve cognitive functions in 5XFAD$^{\Delta PPAR\alpha}$ mice (5XFAD mice lacking PPARα). On the other hand, treadmill workout increased ADAM10, decreased plaque pathology and protected memory and learning in 5XFAD$^{\Delta PPAR\beta}$ mice (5XFAD mice lacking PPARβ). Moreover, the other PPAR (PPARγ) also did not play any role in the transcription of ADAM10 *in vivo* in the hippocampus of treadmill exercised 5XFAD mice. These results underline an important role of PPARα in which treadmill exercise remains unable to exhibit neuroprotection in the hippocampus in the absence of PPARα.

Graphical Abstract

Address correspondence: Kalipada Pahan, Ph.D., Division of Research and Development, Jesse Brown Veterans Affairs Medical Center, Chicago, USA, Tel: (312) 563-3592, Fax: (312) 563-3571, Kalipada_Pahan@rush.edu.

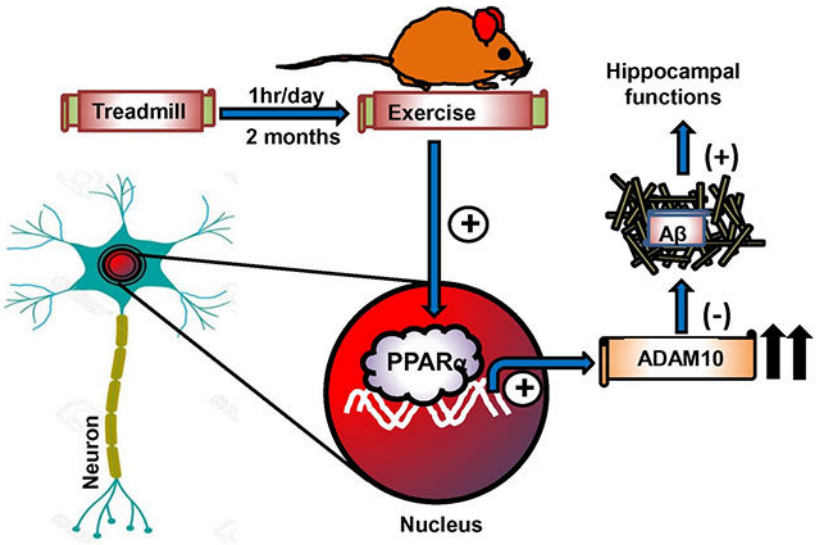

Introduction

Alzheimer's disease (AD) is the most prevalent neurodegenerative disease and constitutes approximately two-thirds of all cases of dementia (Reitz et al., 2011). AD is pathologically characterized by amyloid plaque, neurofibrillary tangles and loss of synapses in the brain. These hallmarks of AD are mostly evident in the cortex and hippocampus (Braak and Braak, 1991; Selkoe, 1993) and it progressively impairs memory, judgment, decision making and language (Nussbaum and Ellis, 2003). Although the precise physiologic changes that trigger development of AD remain unknown, abnormal metabolism of the type 1 transmembrane amyloid precursor protein (APP) into amyloid-β plays a causative role in AD (LaFerla et al., 2007).

Several proteases have been suggested as AD-relevant α-secretases, many of which belong to the ADAM (a disintegrin and metalloproteinase) family of widely expressed, transmembrane and secreted proteins including ADAM9, ADAM10 and ADAM17 of approximately 750 amino acid length (Huovila et al., 2005). In general, these proteins having Zn^{2+} sheddase activity are involved in cell adhesion and proteolytic processing of the ectodomains of diverse cell-surface receptors and signaling molecules (Huovila et al., 2005; Seals and Courtneidge, 2003). Amongst, ADAM10 has emerged as the constitutive and inducible APP α-secretase in neurons (Kuhn et al., 2010). Studies on AD research evidenced that neuron-specific overexpression of ADAM10 decreases Aβ load in a mouse model of AD (Postina et al., 2004), and impaired ADAM10 trafficking to the synapse generates a model of sporadic AD (Epis et al., 2010). In human studies, deficits in ADAM10 expression (Colciaghi et al., 2004), trafficking (Marcello et al., 2013), and activity (Colciaghi et al., 2002) have been observed in AD patients, highlighting that dysregulation of ADAM10 plays a fundamental role in the establishment of Aβ pathology. Therefore, attempts to upregulate the ADAM10 α-secretase expression may be crucial to delineate new therapeutic approaches on the clearance of Aβ plaque burden in AD.

Despite intense investigations, effective or disease-modifying therapies for AD are still lacking. Recently, treadmill exercise has emerged as a non-pharmacologic approach to exert positive effects in the brain. While in one hand, treadmill workout upregulates the neurotrophic factors (viz., BDNF and GDNF) to maintain the normal brain activity (Fang et al., 2013; Xiong et al., 2015), it also improves the memory and cognitive functions (Moore et al., 2016; Thomas et al., 2020; Xiong et al., 2015). Some studies have also shown that treadmill running alleviates Aβ deposition (Koo et al., 2017; Thomas et al., 2020). However, according to Zhao et al (Zhao et al., 2015), treadmill run is unable to lower Aβ pathology in hippocampi of APP/PS1 mice.

In the present study, we demonstrated that treadmill workout upregulated α-secretase ADAM10, but neither BACE1 nor PSEN1, and reduced the level of Aβ plaques *in vivo* in the hippocampus of 5XFAD transgenic (Tg) mouse model of AD. While studying underlying mechanisms, we found that treadmill exercise upregulated PPARα to stimulate the transcription of *ADAM10 in vivo* in the hippocampus, leading to the reduction of endogenous Aβ production by shifting APP processing towards the non-amyloidogenic α-secretase pathway. Peroxisome proliferator-activated receptors (PPARs) are a group of nuclear hormone receptor family transcription factors that are known to control metabolism of lipids and glucose, energy metabolism, adipogenesis, etc. (Marcus et al., 1993). Here, we demonstrate that treadmill exercise remained unable to upregulate ADAM10, decrease plaques and improve memory in Tg mice lacking PPARα, but not PPARβ, highlighting an important role of PPARα in treadmill exercise-mediated beneficial effects in the hippocampus.

Materials and methods

Reagents

Cy2- and Cy5-conjugated secondary antibodies were obtained from Jackson Immuno-Research Laboratories (West Grove, PA). Details about primary antibodies are given in Table S1.

Animals: 5XFAD [(APPwFILon, PSEN1*M146L*L286V)6799Vas/J-transgenic] mice, referred to here as transgenic or Tg, were purchased from the Jackson laboratory (Chakrabarti et al., 2021; Modi et al., 2015). Non-transgenic (Non-Tg) mice generated during breeding and genotyping of 5XFAD mice were also allowed to age to be used as age- and background-matched controls for 5XFAD mice in experiments. PPARα$^{-/-}$ mice were purchased from the Jackson laboratory. PPARβ$^{-/-}$ mice, kindly provided by Dr. Frank Gonzalez of National Institutes of Health, are also present in our lab (Ghosh et al., 2012; Ghosh et al., 2015; Jana et al., 2012). 5XFAD$^{\Delta PPAR\alpha}$ mice (5XFAD mice lacking PPARα), referred here as Tg$^{\Delta PPAR\alpha}$ mice, were developed earlier in our lab (Corbett et al., 2015). These mice were maintained Tg for the 5XFAD mutations and homozygous for the *PPARα* null allele through genotyping (Patel et al., 2018; Patel et al., 2020b). Mice were housed in a specific pathogen-free state-of-the art animal care facility of the Cohn Research Building of the Rush University Medical Center at 72°F with a 12 h light/12 h dark cycle and 50% humidity. Food and water were available *ad libitum*. Daily veterinary care were provided to

all animals by the Vivarium staff under the supervision of the attending veterinarian, Jeffrey P. Oswald, DVM, DACLAM. Animals care and experiments were performed in accordance with National Institutes of Health guidelines and were approved (protocol # 18-045) by the Rush University Medical Center Institutional Animal Care and Use Committee. Six-month-old male and female mice were used for experiments.

Treadmill running exercise

Treadmill exercise was carried out as described (Choi et al., 2021; Koo et al., 2017; Zhao et al., 2015) with minor modifications. Briefly, before starting the treadmill running exercise, all mice were transferred to animal behavior study room separated from the main animal housing facility. All animals were kept in this room during the exercise procedures in order to minimize environmental disruptions among the mice not subjected to the exercise protocol. Moreover, during treadmill exercise, each mouse was housed in a separate cage. Mice in the treadmill exercise group (TE group) received one-week of habituation period to familiarize in the treadmill environment. Since six-month-old 5XFAD (Tg) mice with established plaque pathology were used for the experiment, mice were allowed to run on treadmill for 2 months. During the habituation period, mice were gently trained to learn how to run on a rotating belt of a motorized treadmill (IITc Life Sciences-800 Series Treadmill Ltd), a digitally controlled unit with high degree of repeatability. Mice performed the following speed sequences daily: 5m/min for 5 min, 6m/min for 5min, 8m/min for 60 min, and reduced gradually to 5m/min for 5 min at the end of exercise protocol. Mice in non-treadmill exercise control group (TC groups) were placed on a static treadmill for the same amount of time. If needed, to encourage mice to run on treadmill, mice were gently pushed with a small stick. In some cases, mice were forced to run on treadmill belt by a transient and mild electrical stimulation constantly delivered from the fixed stainless-steel bars located at the beginning of treadmill platform. However, despite 7 days of trials, whenever any mouse was receiving repeated electrical stimulation (more than one per day) or trying to take rest on the side, it was excluded from the exercise procedure. As a result, a total of 12 mice from all different groups were excluded from the study.

Immunoblotting

Western Blot experiment was performed as described previously (Ghosh et al., 2012; Ghosh et al., 2015). Briefly, the mice were euthanized, and hippocampus region with coordinates −1.5 mm AP and −1.5 mm ML was rapidly dissected from the brain on ice after treadmill exercise. The weight of tissue (25 mg) was measured and then stored at −80°C until the assay. Tissue was dissolved and homogenized in buffer (RIPA buffer or CHAPS buffer) containing protease and phosphatase inhibitors (Sigma) on ice, followed by a spin of 30 min/15000 rpm at 4°C. The supernatant was then collected and analyzed for protein concentration by using the Bradford method (Bio-Rad). Next, SDS sample buffer was added to 30–50 μg of total protein and boiled for 5 min. Denatured samples were electrophoresed on custom-made SDS-polyacrylamide gels (10%–15%) or NuPAGE Novex 4–12% Bis-Tris gels (Invitrogen) using the Tris/Glycine/SDS buffer, followed by the proteins transferred onto a nitrocellulose membrane (Bio-Rad) using the Thermo-Pierce Fast Semi-Dry Blotter. Following the transfer of proteins, the membrane was then washed for 15 min in PBS plus 0.1% Tween-20 (PBST) and blocked for 1 hour with blocking buffer (Li-Cor Biosciences).

Later, the membranes were incubated overnight 4°C under shaking condition with primary antibodies (Table S1). The next day, membranes were washed in PBST (3 washes 10 min each) and incubated in secondary antibodies for 1 hour at room temperature. Following washes in PBST, membranes were visualized under the Odyssey Infrared Imaging System (Li-Cor, Lincoln, NE).

Densitometric analysis.—Densitometric quantification of the immunoblots was performed using ImageJ (NIH, Bethesda, MD) as described before (Dutta et al., 2021). Protein bands were normalized using their respective β-Actin loading controls. Data are representative of the average fold change with respect to control.

Immunohistochemistry (IHC).—Following the treadmill running exercise, mice were anesthetized and perfused intracardially with ice-cold PBS and then with 4% paraformaldehyde solution in 0.1M phosphate buffer, pH 7.4. The brains were dissected, labeled and post-fixed in paraformaldehyde overnight at 4°C. Next day, the brains were stored in phosphate buffer containing 30% sucrose at 4°C. Then the brains were cut, and hippocampal sections were saved in serial order at −20°C until immunostained as described previously (Ghosh et al., 2007; Ghosh et al., 2009; Raha et al., 2021a).

IHC using the fluorescence microscopy.—It was performed as described (Chandra et al., 2018; Patel et al., 2018). Briefly, the half brains were incubated with 4% paraformaldehyde, followed by incubation in 30% sucrose overnight at 4°C. Brains were then embedded in optimal cutting temperature medium (Tissue Tech) at −80°C and processed for conventional cryosectioning. Free floating brain sections (40 μm thickness) were initially washed with PBSTT (PBS + 0.1% Triton X + 0.1% Tween-20) and blocking with 2% BSA in PBSTT for 1 hour at room temperature. Sections were incubated with double labeling primary antibodies at 4°C overnight under shaking condition. Next day, sections were washed again with PBSTT and were further incubated with Cy_2 and Cy_5 (Jackson ImmunoResearch Laboratories, Inc.) conjugated secondary antibody for 1 hour at room temperature. Following washes in PBSTT, the stained sections were mounted on gelatin-coated slides and allowed to air-dry. The slides were then rehydrated in double distilled water and then gradually dehydrated in successive baths of ethanol (i.e., 50%, 70%, 90%, 95% and 100%). Finally, the slides were given two baths in 100% xylenes, cover-slipped and dried in dark hood.

The Aβ plaques in brain tissue were detected by thioflavin-S staining as described before (Chandra et al., 2018; Chandra et al., 2019a; Raha et al., 2021b). In thioflavin-S and amyloid-β 6E10 co-labeling, following the primary and secondary antibody incubation for 6E10, sections were incubated in 0.05% thioflavin-S for 5 min. The sections were then washed in 50% ethanol and PBS followed by the mounting on a glass slide. Next, the sections were allowed to air-dry in dark hood and visualized under an Olympus-BX41 fluorescence microscope.

IHC using the light microscopy.—Free-floating brain sections (40 μm thickness) were stained using standard immunohistochemical techniques as described previously (Chandra et al., 2016; Chandra et al., 2017; Dutta et al., 2021). Following washes in

dilution media, sections were incubated with sodium meta-periodate in Tris-buffer to block endogenous peroxidase for 20 minutes and again washed with dilution media. Sections were blocked in 2% BSA in PBS with 1% horse serum for 60 minutes, followed by overnight incubation with primary antibodies under shaking conditions at 4°C. Next day, sections were washed and incubated with secondary antibody (1:200, biotinylated Vector Laboratories, Burlingame, CA 94010) for 1 hour at room temperature, followed by washing with dilution media. Vectastain Elite ABC peroxidase kit (Vector laboratories) was used for visualization using 0.06% 3,3'-diaminobenzidine (Sigma) and H_2O_2. Sections were then mounted on gelatin-coated glass slides and allowed to air-dry. The slides were then rehydrated in double distilled water and gradually dehydrated in successive baths of ethanol (i.e., 50%, 70%, 90%, 95% and 100%). The slide was given two baths in 100% xylenes, cover-slipped and dried at room temperature. Stained sections were viewed and photographed using a Nikon Olympus BX61-VCB microscope.

Estimation of hippocampal volume

Hippocampal volume was measured using the Cavalieri estimator as described previously (Redwine et al., 2003; Yuede et al., 2009). Briefly, we used Stereo Investigator software (Micro-BrightField, Williston, VT) driving a motorized stage on a Zeiss Axioplan 2ie on NeuN-immunostained sections. The section thickness was empirically determined in each tissue sections and average of sections was calculated. Then the area of interest was generated with contours drawn in stained sections using 1.25 × objective and the estimation of the area of interest was performed by means of 50 × 50 μm point grid.

Campbell-Switzer silver staining of Aβ plaques.—After the completion of treadmill running exercise, mice were anesthetized and perfused with ice-cold PBS and then with 4% paraformaldehyde solution in PBS followed by dissection of brain from each mouse for Campbell-Switzer silver staining as described in earlier studies (Lavenir et al., 2019). Briefly, half brains were incubated in 4% paraformaldehyde, followed by 10% sucrose for 3 hours and 30% sucrose overnight at 4°C. Brains were then embedded in optimal cutting temperature medium (Tissue Tech) at −80°C and processed for conventional cryosectioning. Briefly, the sections were incubated in freshly prepared 2% ammonium hydroxide for 5 min. Then, sections were placed in a silver-pyridine-carbonate solution for 40 min, 1% citric acid for 3 min, and 0.5% acetic acid until ready for development. Next, the sections were developed in Physical Developer ABC solution (containing Na carbonate citric acid, tungstosilicic acid and formaldehyde) with the development time being visually assessed. The development was stopped by briefly placing the sections in 0.5% acetic acid. The stained sections were then mounted on gelatinized glass slides and allowed to air-dry. Next, the slides were rehydrated in double distilled water and gradually dehydrated in successive baths of ethanol (i.e., 50%, 70%, 90%, 95% and 100%). Then the slide was given two baths in 100% xylenes, cover-slipped and dried at room temperature. Stained sections were observed and photographed using the Nikon Olympus BX61-VCB microscope and the number, density, size of plaque loads was quantified and compared between the mice with and without treadmill running exercise.

Measurement of Mean fluorescence intensity (MFI).—The MFI measurement was conducted using the "measurement module" of the Microsuite V Olympus software as described (Chakrabarti et al., 2019). Briefly, the images were opened in their specific channel in order to analyze MFI of PPAR α or β or γ in brain. Later, measurement module was opened followed by the selection of two parameters, viz., perimeter and MFI. We outlined a rectangular box to obtain a perimeter and then associated MFI in that obtained perimeter was automatically measured. The MFI was finally analyzed after subtracting the value with the background signal of respective images (Chandra et al., 2018; Rangasamy et al., 2018).

Counting of Aβ plaques.—Amyloid plaques in hippocampus and cortex were counted using the touch-counting module of the Olympus Microsuite V software (Chandra et al., 2018; Raha et al., 2021b). Briefly, captured images were opened in the Infinity image viewer window and the area of the entire image was measured by drawing a rectangular object around the image. Subsequently, the plaques were counted by touch counting. Both area of the image and counted signals were exported in the excel sheet and calculated as a unit of number of signals per square millimeter area.

ELISA for $A\beta_{1-42}$ and $A\beta_{1-40}$.—It was performed as described before (Corbett et al., 2015; Rangasamy et al., 2015). Briefly, hippocampal tissues were homogenized in TBS and pelleted for 30 minutes at 150,000 g. The pellet was resuspended in 3 volumes (w/v original tissues weight) of TBS plus 1% Triton X-100, pelleted for 30 minutes at 150,000 g, and the supernatant recovered stored. Samples were assayed for protein concentration and diluted 10-fold prior to performing ELISA according to the manufacturer's instructions (BioLegend). Sensitivity of both $A\beta_{1-42}$ and $A\beta_{1-40}$ kits is 0.49 ± 0.16 pg/mL.

In situ chromatin immunoprecipitation (ChIP) assay

In situ ChIP was performed as described (Dutta et al., 2021; Paidi et al., 2021). Briefly, animals were perfused with PBS and then PBS containing 4% paraformaldehyde followed by isolation of hippocampus for the isolation of DNA using the phenol–chloroform–isopropyl alcohol method of DNA isolation. ChIP was performed on the cell lysate by overnight incubation at 4 °C with 2 μg of anti-PPARα, anti-CBP or anti-RNA polymerase II antibodies followed by incubation with protein G agarose (Santa Cruz Biotechnology) for 2 h. The beads were then washed with cold IP buffer, and a total of 100 μl of 10% Chelex (10 g/100 ml H_2O) was added to the washed protein G beads and vortexed. The Chelex/protein G bead suspension was boiled for 10 min and then allowed to return to room temperature. Proteinase K (100 μg/ml) was then added, and the beads were incubated for 30 min at 55°C while shaking, followed by another round of boiling for 10 min. The suspension was centrifuged, and the supernatant was collected. This elute was used for conducting semi-quantitative and real-time PCR. The PPRE-containing fragment (205 bp) of the mouse *ADAM10* promoter was amplified using the following primers: sense: 5′-CCCTCAGGATCGATGCACCGCGGTT-3′, antisense: 5'-TGAGAGGTATCATAATCAAGTACTT-3′. For real-time PCR, data were normalized with the input and the fold change with respect to the untreated control was calculated.

Open field behavior test.—This test was conducted as described in our earlier studies (Rangasamy et al., 2019; Rangasamy et al., 2020). Briefly, mice were allowed to move freely to explore an open field arena (i.e., a wooden floor square arena measuring 40×40cm. with walls 30cm high) for 5 min. A video camera 6 (*Basler Gen I Cam – Basler acA 1300-60)* connected to a Noldus computer system was fixed in top facing-down on the center of open field arena. Each mouse was placed individually on center of the arena and the performance of mice was monitored by the live video tracking system. The central area was arbitrarily defined as a square of 20×20cm (half of the total area). Stress-related and exploratory parameters were analyzed that include frequency and time spent at each area (center and corner) and locomotor activity.

Barnes maze test.—Spatial learning and memory was tested by Barnes maze as described previously (Patel et al., 2020b; Rangasamy et al., 2018; Roy et al., 2013). Briefly, mice were trained for 2 consecutive days followed by examination on day 3 in Barnes maze test. During the training session, the overnight food-deprived mouse was placed in the middle of maze within a cylinder start chamber. After 10 seconds, the start chamber was removed to allow the mouse to move around the maze to find out the color food chips in the escape tunnel. The session was ended when the mouse entered the escape tunnel. Then the maze and escape tunnel were thoroughly cleaned with a mild detergent to avoid the ability of animals to use any olfactory clues cognitive influences between the testing session. On day 3, a video camera (*Basler Gen I Cam – Basler acA 1300-60)* connected to a *Noldus* computed system was placed above the maze and was illuminated with high wattage light that generated enough light and heat to motivate animals to enter into the escape tunnel. The performance was monitored by the video tracking system (*Noldus System*). Cognitive parameters were analyzed by measuring latency (duration before all four paws were on the floor of the escape box) and errors (incorrect responses before all four paws were on the floor of the escape box).

T-maze test.—Mice were habituated for 2 days under food-deprived conditions before conducting T-maze test (Patel et al., 2020b; Rangasamy et al., 2018). All the mice received food reward for at least 5 times over a 10-min period of training. During each trial, mice were placed in the starting point for 30s and then forced to make a right arm turn which was always provided with color chips as food reward. On entering the right arm, they were allowed to stay there for 30–45s, then returned to the start point, held for 30s, and then allowed to make right turn again. Between each testing session, T-maze was cleaned with mild detergent solution so as to reduce the animal's ability to use any olfactory clue. On day 3, mice were tested for making positive turns and negative turns. The food-reward side was always associated with a visual cue. Number of times the animal moves to right arm of T-maze and eats the food reward would be considered as a positive turn. Mice were allowed to make 10 trials and the number of positive and negative turns were recorded.

Novel-object recognition (NOR) test.—The NOR test was performed to examine the short-term memory as described before (Rangasamy et al., 2020; Rangasamy et al., 2018). Briefly, during the training period, the mice were placed in an open field arena (i.e., a wooden floor square arena measuring 40×40 cm. with walls 30 cm high). Two plastic

objects (between 2.5 and 3 inches) that varied in color, shape, and texture were placed in specific locations in the environment 18 inches away from each other. A video camera (*Basler Gen I Cam – Basler acA 1300-60)* connected to a *Noldus* computed system was fixed in top facing-down on the center of open field arena. The mice were allowed to explore freely the environment and objects for 15 min and were then placed back into their individual home cages. After 30 min, mice were placed back into the environment with two objects in the same locations, but now one of the familiar objects was replaced with a third novel object. The mice were then again allowed to explore freely both objects for 15 min and the duration spent by the mice towards the novel object was measured. Between each testing session, the objects and open field arena were thoroughly cleaned with a mild detergent so as to avoid the animal's ability to use any olfactory clue.

Statistical analysis.—Based on our previous studies of similar type and complexity, six mice are expected to give > 80% power for all behavioral experiments. Statistical analyses were performed with Student's *t*-test for two-group comparison and one-way ANOVA followed Tukey's multiple comparison tests as appropriate for multiple comparison by using GraphPad Prism 9. Data are represented as mean ± SEM.

Results

Treadmill exercise alters the level of α, β and γ secretases in hippocampus of 5XFAD (Tg) mice.

APP-related secretases play an essential role in the formation of amyloid plaques. Therefore, we investigated the effect of treadmill exercise on the level α-secretases (ADAM10 and ADAM17), β-secretase (BACE1) and the γ-secretase catalytic component presenilin-1 or PSEN1 in the hippocampus of Tg-mice. After removal of the prodomain, enzymatically mature ADAMs are transported to the cell membrane. As a result, membrane fractions are enriched in mature ADAM10 and mature ADAM17. Nondenaturing solubilization of the membrane pellet or the hippocampus as a whole in 1% CHAPS buffer greatly increases the extraction of a truncated, transmembrane C-terminal ADAM10 fragment (ADAM10*CTF*) (Tousseyn et al., 2009). While monitoring these molecules in Tg and age-matched non-Tg mice, we observed decreased levels of pro and mature ADAM10 and ADAM17 as well as ADAM10 CTF in the hippocampus of Tg mice as compared to non-Tg mice (Fig. 1A, B, E, F, G, H, & I). However, 2 months of treadmill exercise markedly restored and/or increased the levels of pro and mature ADAM10 and ADAM17, and ADAM10 CTF in the hippocampus of Tg mice (Fig. 1A, B, E, F, G, H, & I). DAB immunostaining of hippocampal-CA1 (Fig. 1L–N) and cortical (Fig. 1L–N) sections also confirmed the decrease in ADAM10 in the CNS of Tg mice, which increased after treadmill run (Fig. 1L–N). Similar results were seen in dorsal, ventral and DG areas (Fig. S1A–D). In contrast, the levels of BACE1 and PSEN1 increased in the hippocampus of Tg mice as compared to non-Tg mice (Fig. 1C, D, J, & K). Moreover, treadmill run was able to suppress the level of BACE1 and PSEN1 in the hippocampus of Tg mice (Fig. 1C, D, J, & K). Together, these results illustrate that treadmill exercise is capable of upregulating the expression of α-secretases ADAM10 and ADAM17 and decreasing BACE1 and PSEN1 in the CNS of Tg-mice.

Having confirmed that treadmill run upregulates the level of α-secretases and downregulates β- and γ-secretases in Tg mice, we next intended to examine whether treadmill workout could do the same in non-Tg mice as it would have implications to maintaining healthy brains in normal individuals. Therefore, 6-month old non-Tg mice were trained and allowed to perform the running exercise on treadmill for two months followed by monitoring the levels of ADAM10, ADAM17, BACE1, and PSEN1 in the hippocampus. Consistent to that observed in non-Tg mice, treadmill run also increased the expression of both precursor and mature ADAM10 and ADAM17 in the hippocampus (Figure 2 B, G, H). On the other hand, levels of BACE1 and PSEN1 decreased in the hippocampus of non-Tg mice after treadmill run (Figure 2 C, D, I, & J). Together, treadmill exercise is capable of upregulating α secretase and downregulating β and γ secretases in hippocampus of both Tg and non-Tg mice.

Earlier it has been shown that both voluntary and forced exercise increases hippocampal volume in Tg2576 mouse model of AD (Yuede et al., 2009). Therefore, we monitored whether our treadmill paradigm also could increase hippocampal volume in 5XFAD or Tg mice. As monitored using the Cavalieri estimator (Fig. S2A), Tg mice at 8 months of age exhibited reduction ($p < 0.001$) in hippocampal volume as compared to non-Tg mice (Fig. S2B). This result is consistent to that observed in other mouse model of AD (Yuede et al., 2009). However, 2-month of treadmill run significantly ($p < 0.001$) increased hippocampal volume in Tg mice (Fig. S2B).

Treadmill exercise reduces the Aβ burden in the hippocampus of Tg-mice.

Amyloid plaque is a major pathological hallmark of AD, which is demonstrated in Tg mice (Oakley et al., 2006; Corbett et al., 2015). Since treadmill run increased α-secretase and decreased β- and γ-secretases, we examined whether running exercise on treadmill was capable of reducing the load of amyloid plaques from the hippocampus of Tg-mice. Immunoblot analysis of hippocampal tissue homogenates using the 82E1 mAb (Fig. 3A–B) and 6E10 mAb (Fig. S3A–C) showed significantly higher level of Aβ plaques in the hippocampus of Tg-mice compared with non-Tg mice. However, treadmill exercise significantly reduced the level of Aβ with a parallel downregulation of β-CTF in the hippocampus of Tg-mice (Fig. 3A–B & Fig. S3A–C). Later, to examine the Aβ deposition in the brain, we also performed double labeling of hippocampal sections with thioflavin-S (Thio-S), a classic amyloid-binding dye that detects β-pleated sheet of the amyloid plaques and Aβ-specific monoclonal antibody 6E10. Analogous to immunoblot results, there was markedly higher number of Thio-S positive and Aβ immunoreactive plaques in Tg mice without treadmill exercise (Fig. S3D–E). However, running exercise on treadmill was able to ameliorate the plaque load in Tg-mice (Fig. S3D–E). In addition, quantitative analysis of Thio-S staining revealed that treadmill workout led to a significant reduction in the Thio-S positive bodies in the cortex and hippocampus of Tg-mice (Fig. S3F–H). Similar results were noticed with diaminobenzidine staining of hippocampal sections using 82E1 antibody. Briefly, we observed robust amyloid deposition in the hippocampus of Tg mice that decreased after treadmill exercise (Fig. 3C–D). Accordingly, we also noticed marked reduction in the plaque size and density in the hippocampus of Tg mice after treadmill run

(Fig. 3E–F). Collectively, these results demonstrate that treadmill exercise can significantly attenuate the burden of amyloid plaques in the hippocampus region of Tg-mice.

Treadmill exercise upregulates ADAM10 via PPARα in the hippocampus of Tg-mice.

Next, we examined mechanism by which treadmill could upregulate ADAM10 in the hippocampus of Tg mice. Earlier we demonstrated that activation of PPARα upregulates ADAM10 in hippocampal neurons (Chandra et al., 2018; Corbett et al., 2015). Therefore, we tried to explore the role of PPARα in neuroprotective role of treadmill run. Double-labeling of hippocampal and cortical sections with NeuN and PPARα revealed significant decrease in PPARα in cortex and hippocampus of Tg mice as compared to non-Tg mice (Fig. S4A–D). Western blot analysis of hippocampal extracts also corroborated this finding (Fig. S4E–F). However, 2 months treadmill exercise markedly increased the level of PPARα in the CNS of Tg mice (Fig. 2A–F), prompting us to investigate its role. Therefore, we used 5XFAD mice lacking PPARα (abbreviated here as $Tg^{\Delta PPARα}$) for treadmill run. As evident from Western blot analysis, treadmill run increased the levels of pro and mature ADAM10 in the hippocampus of Tg, but not $Tg^{\Delta PPARα}$, mice (Fig. 4A–C). DAB immunostaining of cortical and hippocampal sections with antibodies against ADAM10 also revealed increase in ADAM10 in the CNS of Tg, but not $Tg^{\Delta PPARα}$, mice by treadmill workout (Fig. 4D–F).

Treadmill exercise reduces the amyloid pathology in Tg-mice via PPARα.

Based on the observation that treadmill exercise upregulates the PPARα level and thus triggers the expression of ADAM10 enrichment in hippocampus, we next examined the role of PPARα in amyloid plaque-ΔPPARα lowering effect of treadmill exercise in Tg mice. It is pertinent to point out that Tg mice without treadmill run exhibited markedly more amyloid pathology relative to Tg-mice minus treadmill (Fig. 5), signifying that ablation of PPARα is a contributing factor for driving more amyloidogenesis in these Tg-mice. Both Tg-mice and $Tg^{\Delta PPARα}$ mice were allowed performing running exercise on treadmill for 2 months followed by Western blot analysis of hippocampal extracts. In contrast to Tg-mice, running exercise on treadmill was ineffective in reducing amyloid pathology in $Tg^{\Delta PPARα}$ mice, indirectly PPARα activation by treadmill exercise could be the underlying mechanism behind its amyloid-attenuating effects (Fig. 5A–C).

Double labeling of hippocampal sections with Thio-S and Aβ-6E10 using the monoclonal antibody 6E10 exhibited a similar pattern of results. In contrast to Tg mice, running exercise of $Tg^{\Delta PPARα}$ mice on treadmill did not show any amelioration in amyloid deposition (Fig. 5D–E). Quantitative analysis of Thio-S positive Aβ plaques also revealed no reduction in area (Fig. 5F–G), count (Fig. 5H–I), and size (Fig. 5J–K) of plaques in the hippocampus of $Tg^{\Delta PPARα}$ mice, but not Tg mice, after treadmill run. To confirm further, we also performed Camphell-Switzer Silver staining (Fig. S5A) to demonstrate the characteristics of Aβ plaques in both Tg and $Tg^{\Delta PPARα}$ mice and found decrease in plaques in cortex and hippocampus of Tg mice, but not Tg ΔPPARα mice, after treadmill run. Results were confirmed by quantitative analysis of number (Fig. S5B), density (Fig. S5C) and area (Fig. S5D) of plaques. Overall, these results indicate that treadmill exercise could alleviate amyloid pathology in Tg mice in a PPARα-dependent manner.

Treadmill exercise protects memory in Tg-mice via PPARα.

One of the major therapeutic goals in AD research is to protect the memory and learning. The hippocampus is part of limbic system that regulates the generation of long-term memory and spatial learning. Our Tg-mice model successfully recaps memory deficits, which is one of the major characteristics of AD. Therefore, we analyzed the effect of treadmill exercise on amelioration of memory behavior in Tg-mice. Many studies have previously used PPARα agonists to enhance memory via CREB (Patel et al., 2018; Patel et al., 2020b; Roy et al., 2013; Roy et al., 2016); however, the benefit of treadmill exercise as a "non-pharmacologic" therapeutic strategy on memory improvement at detailed molecular level has not yet studied. After running exercise on the treadmill, memory functions of mice were analyzed by Barnes maze, T-maze, and Novel object recognition test. As reported earlier (Patel et al., 2018; Patel et al., 2020b; Raha et al., 2021b), control Tg mice did not find the reward hole easily as these mice required more time (latency) and made more errors as compared to age-matched non-Tg mice (Fig. S6A–C). However, treadmill exercised Tg mice were as capable as non-Tg control mice in finding the target hole, with less latency and fewer errors (Fig. S6A–C). Likewise, Tg mice without treadmill run exhibited a lower number of positive turns and a higher number of negative turns than non-Tg mice in T-maze test (Fig. S6D–E). However, we noticed that Tg mice with treadmill exercise exhibited significantly more positive turns and less negative turns than Tg mice without exercise (Fig. S6D–E). These results delineate the beneficial effect of treadmill exercise in improving spatial learning and memory in Tg mice. Similarly, we also examined short-term memory by novel-object recognition test as described before (Rangasamy et al., 2018). This task mainly used to evaluate cognition behavior and it requires no external motivation, reward or punishment and completed in a shorter period with minimal stress. Tg-mice without any exercise showed profound impairment in short-term memory as evidenced by novel-object exploration time as compared to age-matched non-Tg mice (Fig. S6F–G). Conversely, we noticed significant improvement in this memory test in Tg-mice following treadmill exercise (Fig. S6F–G).

Next, we examined whether treadmill exercise-mediated recovery of memory functions is dependent on PPARα by comparing the memory behavior between Tg-mice and $Tg^{\Delta PPAR\alpha}$ mice after treadmill workout. Although treadmill exercise recovered or improved spatial learning and memory of Tg-mice, it did not show any improvement for $Tg^{\Delta PPAR\alpha}$ mice as evident from Barnes maze and T-maze (Fig. S6A–E). Similarly, in novel-object recognition test as well, no such improvement in this behavior was noticed in $Tg^{\Delta PPAR\alpha}$ mice upon treadmill exercise (Fig. S6F–G). Later, we examined the general locomotor functions of different groups of mice by open field behavior test and found no significant difference in velocity (Fig. S6H) of these mice, indicating that the enhancement of memory functions is specific and not due to any effect on motor activity of these groups of mice. Collectively, the results of this study delineate that treadmill run improves cognitive functions of Tg-mice via PPARα.

Treadmill exercise does not need PPARβ to upregulate ADAM10 and reduce amyloid pathology in Tg mice.

Similar to PPARα, PPARβ is also present in the brain to play a role in different brain activities including myelination (Jana et al., 2012). Therefore, next, we examined the

role of PPARβ in neuroprotective effects of treadmill exercise. First, we studied whether treadmill exercise upregulated the expression of PPARβ in hippocampus region of Tg-mice. Immunofluorescence staining of hippocampal and cortical sections as well as immunoblot analysis of hippocampal tissue extracts for PPARβ demonstrated that in contrast to PPARα, the level of PPARβ did not decrease in the CNS of Tg mice as compared to non-Tg mice (Fig. S7A–E). Moreover, treadmill exercise remained unable to modulate PPARβ in the hippocampus of Tg-mice (Fig. S7A–E). Next, to further investigate the role of PPARβ, we generated $Tg^{\Delta PPAR\beta}$ mice (5XFAD mice lacking PPARβ) via breeding 5XFAD mice with PPARβ null mice (Fig. S8). Primers for genotyping $Tg^{\Delta PPAR\beta}$ mice are given in Table S2. Although treadmill workout did not increase the level of ADAM10 in the hippocampus of $Tg^{\Delta PPAR\alpha}$ mice (Fig. 4), similar to Tg mice, we found upregulation in both pro and mature ADAM10 in the hippocampus of $Tg^{\Delta PPAR\beta}$ mice after treadmill run (Fig. S9A–C), suggesting that treadmill run does not require PPARβ to upregulate ADAM10 in the hippocampus of Tg mice.

Next, we examined the role of PPARβ in plaque lowering effect of treadmill. We performed DAB staining of hippocampal sections using the 6E10 mAb to demonstrate the features of amyloid plaque pathogenesis in Tg and $Tg^{\Delta PPAR\beta}$ mice with or without treadmill exercise. Similar to Tg mice, in $Tg^{\Delta PPAR\beta}$ mice as well, we noticed numerous dense-cored amyloid plaques in hippocampus (Figure S10A). Quantitative analysis of amyloid plaques also revealed that number, area and density of plaques in the hippocampus of Tg mice is very much similar to that in $Tg^{\Delta PPAR\beta}$ mice (Fig. S10B–D). Moreover, dissimilar to that found in $Tg^{\Delta PPAR\alpha}$ mice, treadmill exercise led to significant decrease in size, density, and number of Aβ plaques in the hippocampus of $Tg^{\Delta PPAR\beta}$ mice (Fig. S10A–D). To further confirm these finding, we performed ELISA of serum and hippocampal extracts for Aβ1-40 and Aβ1-42. ELISA of serum (Fig. S11A–B), TBS-extracted hippocampal fractions (Fig. S11C–D), and (TBS plus 1% Triton X-100)–extracted hippocampal fractions (Fig. S11E–F) revealed a marked increase in Aβ1-40 and Aβ1-42 in Tg mice compared with non-Tg mice. However, treadmill run decreased the levels of Aβ1-40 and Aβ1-42 in serum, TBS-extracted hippocampal fractions, and (TBS plus 1% Triton X-100)–extracted hippocampal fractions of Tg and $Tg^{\Delta PPAR\beta}$ mice, but not $Tg^{\Delta PPAR\alpha}$ mice (Fig. S11A–F). Together, these results suggest that treadmill run lowers amyloid plaques via PPARα, but not PPARβ.

Treadmill exercise does not depend on PPARβ to improve cognitive functions in Tg mice.

Next, we next examined whether treadmill exercise involved PPARβ to protect hippocampus related behavioral functions in Tg mice. Following treadmill exercise, cognitive functions of these mice were evaluated by Barnes maze, T-maze and novel object recognition tests. In contrast to that found in $Tg^{\Delta PPAR\alpha}$ mice and similar to Tg mice, treadmill run improved cognitive performances of $Tg^{\Delta PPAR\beta}$ mice as demonstrated by track plot (Fig. S12A), latency (Fig. S12B) and errors (Fig. S12C) on Barnes maze, positive turns (Fig. S12D) and negative turns (Fig. S12E) on T-maze, and track plot (Fig. S12F) and exploration time (Fig. S12G) on novel object recognition tests. Again, these results were not influenced by any change in locomotor activities in either Tg mice or $Tg^{\Delta PPAR\beta}$ mice as monitored by open-field behavior such as velocity (Fig. S12H). Therefore, although PPARβ plays many roles in the CNS, it does not participate in treadmill workout-mediated upregulation

of ADAM10, reduction of amyloid pathology and improvement in cognitive functions in 5XFAD mouse model of AD.

Treadmill exercise upregulates the expression of PPARγ in the hippocampus of Tg-mice.

Having studied the effect of treadmill exercise on PPARα and PPARβ level, we next proposed to analyze whether similar exercise could alter the expression of PPARγ in the CNS of Tg-mice. As apparent from immunofluorescence scrutiny of cortical and hippocampal sections and Western blot analysis of hippocampal extracts, the level of PPARγ decreased in the hippocampus of Tg mice as compared to non-Tg mice (Fig. S13A–E). However, similar to the modulation of PPARα and in contrast to that found for PPARβ, 2 months of treadmill exercise significantly increased and/or restored the level of PPARγ in the CNS of Tg mice (Fig. S13A–E).

Treadmill exercise stimulates the recruitment of PPARα, but neither PPARβ nor PPARγ, to *ADAM10* gene promoter *in vivo* in the hippocampus of Tg mice.

Since treadmill run upregulated the level of ADAM10 in the hippocampus of Tg mice via PPARα, but not PPARβ, and treadmill run was also capable of increasing the expression of PPARγ, we examined whether PPARα, PPARβ and PPARγ were directly involved in treadmill exercise-mediated transcription of ADAM10 gene *in vivo* in the hippocampus. After 2 months of treadmill exercise of both non-Tg mice and Tg mice, we examined the recruitment of PPARα, PPARβ and PPARγ to the *ADAM10* gene promoter *in vivo* in the hippocampus by *in situ* ChIP assay. One consensus PPRE is present in the *ADAM10* gene promoter very close to the transcription start site (Fig. 7A). After immunoprecipitation of chromatin fragments by antibodies against PPARα, we were able to amplify a 205 bp DNA portion encompassing the PPRE of the *ADAM10* promoter in hippocampus of non-Tg mice (Fig. 7A, B & D). On the other hand, we could not amplify any DNA piece from chromatin fragments of non-Tg hippocampus after immunoprecipitation with antibodies against either PPARβ or PPARγ (Fig. 7B & D), suggesting that PPARα, but neither PPARβ nor PPARγ, is enrolled to the *ADAM10* promoter *in vivo* in the hippocampus of non-Tg mice. However, the enrollment of PPARα to the *ADAM10* promoter markedly decreased in the hippocampus of Tg mice as compared to non-Tg mice (Fig. 7D & E). Interestingly, treadmill exercise increased the recruitment of PPARα to the *ADAM10* promoter *in vivo* in the hippocampus of both non-Tg and Tg mice (Fig. 7B–E). On the other hand, although treadmill run increased the level of PPARγ in the hippocampus, we did not find any increase in PPARγ staffing to the *ADAM10* promoter in either non-Tg or Tg mice after treadmill (Fig. 7B–E). Treadmill run also did not induce or stimulate the enrollment of PPARβ to the ADAM10 promoter (Fig. 7B–E). However, similar to the recruitment of PPARα, we observed decreased employment of CREB-binding protein (CBP), an important histone acetyl transferase, and RNA polymerase in the *ADAM10* promoter in the CNS of Tg mice, which was restored and/or increased by treadmill workout (Fig. 7B–E). These results are specific as no product amplification was observed in immunoprecipitants with control IgG. Together, these results indicate that treadmill exercise increases the recruitment of PPARα, but neither PPARβ nor PPARγ, to the *ADAM10* promoter *in vivo* in the hippocampus of Tg mice.

Discussion

Buildup of the amyloid-β (Aβ) peptide in the brain is possibly the early event in the disease process of AD. It is believed that the accumulation of Aβ starts 15–20 years before the onset of clinical symptoms. Although over the past two and half decades, we have seen intense investigations for decreasing aggregated plaques and different forms of Aβ, these approaches have failed to show clinical benefit in large clinical trials involving AD patients. Mainly, three different mechanisms of action have been tested for plaque lowering: *First,* inhibitors of β and γ secretases for reducing the production of Aβ. *Second,* active or passive immunotherapy for promoting Aβ clearance that created massive enthusiasm among patients, caregivers and associated industries. *Third,* drugs to reduce Aβ plaque burden via disruption of aggregates or inhibition of aggregation. Since all three approaches failed in clinical trials, it makes sense to try another line of method. It is known that juxtamembrane cleavage of APP between K16/L17 residues by α-secretase ADAM10 prevents Aβ generation (Allinson et al., 2003). Compared to above three failed approaches, this α-secretase-mediated non-amyloidogenic strategy received less attention both preclinically and clinically. In this respect, it is important to mention that treadmill exercise, an absolutely drug-free approach, is capable of upregulating the α-secretase pathway in both plaque-free aged control mice and plaque containing 5XFAD Tg mice. Although there was no plaque in control mice, regular treadmill exercise upregulated ADAM10 and decreased BACE1 and PSEN1 in the hippocampus, suggesting that treadmill workout may be an easy solution for preventing amyloid deposition in older individuals. In plaque-containing Tg mice as well, treadmill run modulated the secretases in the same way, leading to decrease in plaque load in the hippocampus, increase in hippocampal volume and improvement in memory and learning, indicating that treadmill exercise may have therapeutic implications in mild to moderate AD patients. While laboratory mice can run as fast as 1.68 m/sec or 100 m/min (Garland et al., 1995), in our treadmill schedule, mice were allowed to run at a speed of only 8 m/min for 60 min. Therefore, it should be considered as a mild jogging regimen for 60 min if translated to human beings. However, our treadmill regimen does not differentiate between voluntary and forced approaches as mice unwilling to run were either encouraged to run by gently pushing with a small stick or forced to run on treadmill by a transient and mild electrical stimulation.

Next, we investigated mechanisms by which treadmill workout exhibited beneficial effects in Tg mice. Peroxisome proliferator-activated receptor (PPAR) is a group of three transcription factors in which three isotypes (PPARα, PPARβ/δ and PPARγ) differ from each other in terms of their physiological functions and tissue distributions (Chandra et al., 2019b; Gottschalk et al., 2021; Marcus et al., 1993; Patel et al., 2020a). While PPARγ is mainly expressed in white and brown adipose tissue controlling adipogenesis, energy balance, lipid biosynthesis, and inflammation (Murphy and Holder, 2000), PPARβ/δ is abundant in the liver, adipose tissue, and skeletal muscle, regulating fatty acid oxidation, mainly in skeletal and cardiac muscles (Magadum and Engel, 2018). On the other hand, liver, heart and kidney, tissues using fat as an energy source, are very rich in PPARα (Keller et al., 1993). Accordingly, PPARα is involved in the transcription of genes responsible for the metabolism of fatty acid (Roy and Pahan, 2009, 2015). However, we have seen the

presence of PPARα in hippocampus and different parts of the brain (Corbett et al., 2015; Roy et al., 2013; Roy et al., 2015; Roy et al., 2021; Roy and Pahan, 2015). Our lab has also demonstrated that PPARα is involved in nonamyloidogenic metabolism of APP in hippocampal neurons via direct transcriptional regulation of *ADAM10* (Corbett et al., 2015). Therefore, we investigated the role of PPARα in treadmill workout-mediated upregulation ADAM10. The level of PPARα decreased in the hippocampus of Tg mice as compared to age-matched non-Tg, which was increased and/or normalized after treadmill exercise. Similar distribution was observed for PPARγ. On the other hand, the level of PPARβ neither decreased in Tg mice without treadmill nor increased after treadmill workout, suggesting that unlike PPARα and PPARγ, PPARβ/δ was not responsive to treadmill run. However, treadmill exercise stimulated the recruitment of PPARα, but neither PPARδ nor PPARγ, to the *ADAM10* gene promoter *in vivo* in the hippocampus of Tg mice. In the hippocampus of non-Tg mice as well, treadmill workout encouraged the recruitment of PPARα, but neither PPARδ nor PPARγ, to the *ADAM10* gene promoter. One study has reported that treadmill exercise can upregulate ADAM10 in APP/PS1 mice (Zhang et al., 2019). However, mechanism remained unknown. Our results suggest although treadmill exercise increases the level of both PPARα and PPARγ, only PPARα is involved in the transcription of *ADAM10* gene *in vivo* in the hippocampus. This finding was verified in $Tg^{\Delta PPAR\alpha}$ animals where in the absence of functional PPARα, there was no up-regulation of ADAM10 in the hippocampus after treadmill exercise. On the other hand, treadmill run increased ADAM10 in the hippocampus of $Tg^{\Delta PPAR\beta}$ mice, Tg mice that lack PPARβ. Accordingly, treadmill run lowered plaque load in the hippocampus of Tg mice and $Tg^{\Delta PPAR\beta}$ mice, but not $Tg^{\Delta PPAR\alpha}$ mice. Together, these results indicates that activation of the PPARα-ADAM10 pathway is probably the underlying reason behind treadmill-induced plaque lowering.

The final goal of plaque lowering therapy or any neuroprotective therapy in AD is to improve cognitive behaviors and it is nice to see that treadmill workout protects memory and learning in Tg mice. Although according to Zhao et al (Zhao et al., 2015), treadmill exercise does not lower Aβ pathology in the hippocampus, but enhances synaptic plasticity, in APP/PS1 mice, Choi et al (Choi et al., 2021) have shown that treadmill exercise improves brain iron homeostasis to reduce cognitive decline and Aβ-induced neuronal cell death in APP-C105 mice. On the other hand, in our study, similar to plaque lowering, treadmill run improves cognitive behaviors of 5XFAD (Tg) mice and $Tg^{\Delta PPAR\beta}$ mice, but not $Tg^{\Delta PPAR\alpha}$ mice, indicating that treadmill workout requires PPARα, but not PPARβ, for upregulating memory and learning in Tg mice. While decrease in plaque alone from the hippocampus can improve hippocampal functions, PPARα has been found to control another pathway to regulate memory and learning. The cAMP response element-binding protein (CREB) plays an important role in synaptic plasticity in the brain (Roy and Pahan, 2015). Our lab has shown that CREB promoter harbors a consensus peroxisome proliferator response element (PPRE) and that activation of PPARα promotes hippocampal plasticity via transcriptional upregulation of CREB (Roy et al., 2013). Therefore, it is possible that PPARα activated in the hippocampus by treadmill run may improve memory and learning via upregulation of CREB. It has been also reported that treadmill exercise improves spatial learning and memory deficits possibly via increasing the level of CREB (Sabouri et al., 2020). Although Del Din et al (Del Din et al., 2020) have described that fall risk in relation to activity

exposure is higher in Parkinson's disease patients than individuals with mild cognitive impairments, since PPARα activation is key for treadmill-mediated neuroprotection, ligands of PPARα (e.g. gemfibrozil) may also be considered for high risk older adults.

In summary, we have seen that treadmill workout increases PPARα in the hippocampus, leading to the upregulation of ADAM10, decrease in plaque load, and protection and/or improvement of memory and learning in in a mouse model of AD. Therefore, treadmill workout-mediated PPARα activation in the hippocampus may be beneficial for increasing ADAM10, lowering plaque formation and improving cognitive functions in AD patients. However, it is to be noted that treadmill run in incapable of exhibiting any beneficial effect on the upregulation of ADAM10, decrease in cerebral plaque load and improvement in memory and learning in Tg mice in the absence of PPARα, underlining an important role of PPARα in these processes.

Supplementary Material

Refer to Web version on PubMed Central for supplementary material.

Acknowledgement

This study was supported by merit awards (BX003033 and BX005002) from US Department of Veterans Affairs and grants (AT010980-01S1 and AG050431) from NIH. Moreover, Dr. Pahan is the recipient of a Research Career Scientist Award (1IK6 BX004982) from the Department of Veterans Affairs.

References

Allinson TM, Parkin ET, Turner AJ, Hooper NM, 2003. ADAMs family members as amyloid precursor protein alpha-secretases. J Neurosci Res 74, 342–352. [PubMed: 14598310]

Braak H, Braak E, 1991. Neuropathological stageing of Alzheimer-related changes. Acta Neuropathol 82, 239–259. [PubMed: 1759558]

Chakrabarti S, Prorok T, Roy A, Patel D, Dasarathi S, Pahan K, 2021. Upregulation of IL-1 Receptor Antagonist by Aspirin in Glial Cells via Peroxisome Proliferator-Activated Receptor-Alpha. J Alzheimers Dis Rep 5, 647–661. [PubMed: 34632302]

Chakrabarti S, Roy A, Prorok T, Patel D, Dasarathi S, Pahan K, 2019. Aspirin up-regulates suppressor of cytokine signaling 3 in glial cells via PPARalpha. J Neurochem 151, 50–63. [PubMed: 31273781]

Chandra G, Rangasamy SB, Roy A, Kordower JH, Pahan K, 2016. Neutralization of RANTES and Eotaxin Prevents the Loss of Dopaminergic Neurons in a Mouse Model of Parkinson Disease. J Biol Chem 291, 15267–15281. [PubMed: 27226559]

Chandra G, Roy A, Rangasamy SB, Pahan K, 2017. Induction of Adaptive Immunity Leads to Nigrostriatal Disease Progression in MPTP Mouse Model of Parkinson's Disease. J Immunol 198, 4312–4326. [PubMed: 28446566]

Chandra S, Jana M, Pahan K, 2018. Aspirin Induces Lysosomal Biogenesis and Attenuates Amyloid Plaque Pathology in a Mouse Model of Alzheimer's Disease via PPARalpha. J Neurosci 38, 6682–6699. [PubMed: 29967008]

Chandra S, Roy A, Jana M, Pahan K, 2019a. Cinnamic acid activates PPARalpha to stimulate Lysosomal biogenesis and lower Amyloid plaque pathology in an Alzheimer's disease mouse model. Neurobiol Dis 124, 379–395. [PubMed: 30578827]

Chandra S, Roy A, Patel DR, Pahan K, 2019b. PPARalpha Between Aspirin and Plaque Clearance. J Alzheimers Dis 71, 389–397. [PubMed: 31424405]

Choi DH, Kwon KC, Hwang DJ, Koo JH, Um HS, Song HS, Kim JS, Jang Y, Cho JY, 2021. Treadmill Exercise Alleviates Brain Iron Dyshomeostasis Accelerating Neuronal Amyloid-beta Production,

Neuronal Cell Death, and Cognitive Impairment in Transgenic Mice Model of Alzheimer's Disease. Mol Neurobiol 58, 3208–3223. [PubMed: 33641078]

Colciaghi F, Borroni B, Pastorino L, Marcello E, Zimmermann M, Cattabeni F, Padovani A, Di Luca M, 2002. [alpha]-Secretase ADAM10 as well as [alpha]APPs is reduced in platelets and CSF of Alzheimer disease patients. Mol Med 8, 67–74. [PubMed: 12080182]

Colciaghi F, Marcello E, Borroni B, Zimmermann M, Caltagirone C, Cattabeni F, Padovani A, Di Luca M, 2004. Platelet APP, ADAM 10 and BACE alterations in the early stages of Alzheimer disease. Neurology 62, 498–501. [PubMed: 14872043]

Corbett GT, Gonzalez FJ, Pahan K, 2015. Activation of peroxisome proliferator-activated receptor alpha stimulates ADAM10-mediated proteolysis of APP. Proc Natl Acad Sci U S A 112, 8445–8450. [PubMed: 26080426]

Del Din S, Galna B, Lord S, Nieuwboer A, Bekkers EMJ, Pelosin E, Avanzino L, Bloem BR, Olde Rikkert MGM, Nieuwhof F, Cereatti A, Della Croce U, Mirelman A, Hausdorff JM, Rochester L, 2020. Falls Risk in Relation to Activity Exposure in High-Risk Older Adults. J Gerontol A Biol Sci Med Sci 75, 1198–1205. [PubMed: 31942969]

Dutta D, Jana M, Majumder M, Mondal S, Roy A, Pahan K, 2021. Selective targeting of the TLR2/MyD88/NF-kappaB pathway reduces alpha-synuclein spreading in vitro and in vivo. Nat Commun 12, 5382. [PubMed: 34508096]

Epis R, Marcello E, Gardoni F, Vastagh C, Malinverno M, Balducci C, Colombo A, Borroni B, Vara H, Dell'Agli M, Cattabeni F, Giustetto M, Borsello T, Forloni G, Padovani A, Di Luca M, 2010. Blocking ADAM10 synaptic trafficking generates a model of sporadic Alzheimer's disease. Brain 133, 3323–3335. [PubMed: 20805102]

Fang ZH, Lee CH, Seo MK, Cho H, Lee JG, Lee BJ, Park SW, Kim YH, 2013. Effect of treadmill exercise on the BDNF-mediated pathway in the hippocampus of stressed rats. Neurosci Res 76, 187–194. [PubMed: 23665137]

Garland T Jr., Gleeson TT, Aronovitz BA, Richardson CS, Dohm MR, 1995. Maximal sprint speeds and muscle fiber composition of wild and laboratory house mice. Physiol Behav 58, 869–876. [PubMed: 8577882]

Ghosh A, Corbett GT, Gonzalez FJ, Pahan K, 2012. Gemfibrozil and fenofibrate, Food and Drug Administration-approved lipid-lowering drugs, up-regulate tripeptidyl-peptidase 1 in brain cells via peroxisome proliferator-activated receptor alpha: implications for late infantile Batten disease therapy. J Biol Chem 287, 38922–38935. [PubMed: 22989886]

Ghosh A, Jana M, Modi K, Gonzalez FJ, Sims KB, Berry-Kravis E, Pahan K, 2015. Activation of peroxisome proliferator-activated receptor alpha induces lysosomal biogenesis in brain cells: implications for lysosomal storage disorders. J Biol Chem 290, 10309–10324. [PubMed: 25750174]

Ghosh A, Roy A, Liu X, Kordower JH, Mufson EJ, Hartley DM, Ghosh S, Mosley RL, Gendelman HE, Pahan K, 2007. Selective inhibition of NF-kappaB activation prevents dopaminergic neuronal loss in a mouse model of Parkinson's disease. Proc Natl Acad Sci U S A 104, 18754–18759. [PubMed: 18000063]

Ghosh A, Roy A, Matras J, Brahmachari S, Gendelman HE, Pahan K, 2009. Simvastatin inhibits the activation of p21ras and prevents the loss of dopaminergic neurons in a mouse model of Parkinson's disease. J Neurosci 29, 13543–13556. [PubMed: 19864567]

Gottschalk CG, Jana M, Roy A, Patel DR, Pahan K, 2021. Gemfibrozil Protects Dopaminergic Neurons in a Mouse Model of Parkinson's Disease via PPARalpha-Dependent Astrocytic GDNF Pathway. J Neurosci 41, 2287–2300. [PubMed: 33514677]

Huovila AP, Turner AJ, Pelto-Huikko M, Karkkainen I, Ortiz RM, 2005. Shedding light on ADAM metalloproteinases. Trends Biochem Sci 30, 413–422. [PubMed: 15949939]

Jana M, Mondal S, Gonzalez FJ, Pahan K, 2012. Gemfibrozil, a lipid-lowering drug, increases myelin genes in human oligodendrocytes via peroxisome proliferator-activated receptor-beta. J Biol Chem 287, 34134–34148. [PubMed: 22879602]

Keller H, Dreyer C, Medin J, Mahfoudi A, Ozato K, Wahli W, 1993. Fatty acids and retinoids control lipid metabolism through activation of peroxisome proliferator-activated receptor-retinoid X receptor heterodimers. Proc Natl Acad Sci U S A 90, 2160–2164. [PubMed: 8384714]

Koo JH, Kang EB, Oh YS, Yang DS, Cho JY, 2017. Treadmill exercise decreases amyloid-beta burden possibly via activation of SIRT-1 signaling in a mouse model of Alzheimer's disease. Exp Neurol 288, 142–152. [PubMed: 27889467]

Kuhn PH, Wang H, Dislich B, Colombo A, Zeitschel U, Ellwart JW, Kremmer E, Rossner S, Lichtenthaler SF, 2010. ADAM10 is the physiologically relevant, constitutive alpha-secretase of the amyloid precursor protein in primary neurons. EMBO J 29, 3020–3032. [PubMed: 20676056]

LaFerla FM, Green KN, Oddo S, 2007. Intracellular amyloid-beta in Alzheimer's disease. Nat Rev Neurosci 8, 499–509. [PubMed: 17551515]

Lavenir I, Passarella D, Masuda-Suzukake M, Curry A, Holton JL, Ghetti B, Goedert M, 2019. Silver staining (Campbell-Switzer) of neuronal alpha-synuclein assemblies induced by multiple system atrophy and Parkinson's disease brain extracts in transgenic mice. Acta Neuropathol Commun 7, 148. [PubMed: 31522685]

Magadum A, Engel FB, 2018. PPARbeta/delta: Linking Metabolism to Regeneration. Int J Mol Sci 19.

Marcello E, Saraceno C, Musardo S, Vara H, de la Fuente AG, Pelucchi S, Di Marino D, Borroni B, Tramontano A, Perez-Otano I, Padovani A, Giustetto M, Gardoni F, Di Luca M, 2013. Endocytosis of synaptic ADAM10 in neuronal plasticity and Alzheimer's disease. J Clin Invest 123, 2523–2538. [PubMed: 23676497]

Marcus SL, Miyata KS, Zhang B, Subramani S, Rachubinski RA, Capone JP, 1993. Diverse peroxisome proliferator-activated receptors bind to the peroxisome proliferator-responsive elements of the rat hydratase/dehydrogenase and fatty acyl-CoA oxidase genes but differentially induce expression. Proc Natl Acad Sci U S A 90, 5723–5727. [PubMed: 8390676]

Modi KK, Roy A, Brahmachari S, Rangasamy SB, Pahan K, 2015. Cinnamon and Its Metabolite Sodium Benzoate Attenuate the Activation of p21rac and Protect Memory and Learning in an Animal Model of Alzheimer's Disease. PLoS One 10, e0130398. [PubMed: 26102198]

Moore KM, Girens RE, Larson SK, Jones MR, Restivo JL, Holtzman DM, Cirrito JR, Yuede CM, Zimmerman SD, Timson BF, 2016. A spectrum of exercise training reduces soluble Abeta in a dose-dependent manner in a mouse model of Alzheimer's disease. Neurobiol Dis 85, 218–224. [PubMed: 26563933]

Murphy GJ, Holder JC, 2000. PPAR-gamma agonists: therapeutic role in diabetes, inflammation and cancer. Trends Pharmacol Sci 21, 469–474. [PubMed: 11121836]

Nussbaum RL, Ellis CE, 2003. Alzheimer's disease and Parkinson's disease. N Engl J Med 348, 1356–1364. [PubMed: 12672864]

Paidi RK, Jana M, Mishra RK, Dutta D, Pahan K, 2021. Selective Inhibition of the Interaction between SARS-CoV-2 Spike S1 and ACE2 by SPIDAR Peptide Induces Anti-Inflammatory Therapeutic Responses. J Immunol 207, 2521–2533. [PubMed: 34645689]

Patel D, Roy A, Kundu M, Jana M, Luan CH, Gonzalez FJ, Pahan K, 2018. Aspirin binds to PPARalpha to stimulate hippocampal plasticity and protect memory. Proc Natl Acad Sci U S A 115, E7408–E7417. [PubMed: 30012602]

Patel D, Roy A, Pahan K, 2020a. PPARalpha serves as a new receptor of aspirin for neuroprotection. J Neurosci Res 98, 626–631. [PubMed: 31797405]

Patel D, Roy A, Raha S, Kundu M, Gonzalez FJ, Pahan K, 2020b. Upregulation of BDNF and hippocampal functions by a hippocampal ligand of PPARalpha. JCI Insight 5.

Postina R, Schroeder A, Dewachter I, Bohl J, Schmitt U, Kojro E, Prinzen C, Endres K, Hiemke C, Blessing M, Flamez P, Dequenne A, Godaux E, van Leuven F, Fahrenholz F, 2004. A disintegrin-metalloproteinase prevents amyloid plaque formation and hippocampal defects in an Alzheimer disease mouse model. J Clin Invest 113, 1456–1464. [PubMed: 15146243]

Raha S, Dutta D, Roy A, Pahan K, 2021a. Reduction of Lewy Body Pathology by Oral Cinnamon. J Neuroimmune Pharmacol 16, 592–608. [PubMed: 32889602]

Raha S, Ghosh A, Dutta D, Patel DR, Pahan K, 2021b. Activation of PPARalpha enhances astroglial uptake and degradation of beta-amyloid. Sci Signal 14, eabg4747. [PubMed: 34699252]

Rangasamy SB, Corbett GT, Roy A, Modi KK, Bennett DA, Mufson EJ, Ghosh S, Pahan K, 2015. Intranasal Delivery of NEMO-Binding Domain Peptide Prevents Memory Loss in a Mouse Model of Alzheimer's Disease. J Alzheimers Dis 47, 385–402. [PubMed: 26401561]

Rangasamy SB, Dasarathi S, Pahan P, Jana M, Pahan K, 2019. Low-Dose Aspirin Upregulates Tyrosine Hydroxylase and Increases Dopamine Production in Dopaminergic Neurons: Implications for Parkinson's Disease. J Neuroimmune Pharmacol 14, 173–187. [PubMed: 30187283]

Rangasamy SB, Ghosh S, Pahan K, 2020. RNS60, a physically-modified saline, inhibits glial activation, suppresses neuronal apoptosis and protects memory in a mouse model of traumatic brain injury. Exp Neurol 328, 113279. [PubMed: 32151546]

Rangasamy SB, Jana M, Roy A, Corbett GT, Kundu M, Chandra S, Mondal S, Dasarathi S, Mufson EJ, Mishra RK, Luan CH, Bennett DA, Pahan K, 2018. Selective disruption of TLR2-MyD88 interaction inhibits inflammation and attenuates Alzheimer's pathology. J Clin Invest 128, 4297–4312. [PubMed: 29990310]

Redwine JM, Kosofsky B, Jacobs RE, Games D, Reilly JF, Morrison JH, Young WG, Bloom FE, 2003. Dentate gyrus volume is reduced before onset of plaque formation in PDAPP mice: a magnetic resonance microscopy and stereologic analysis. Proc Natl Acad Sci U S A 100, 1381–1386. [PubMed: 12552120]

Reitz C, Brayne C, Mayeux R, 2011. Epidemiology of Alzheimer disease. Nat Rev Neurol 7, 137–152. [PubMed: 21304480]

Roy A, Jana M, Corbett GT, Ramaswamy S, Kordower JH, Gonzalez FJ, Pahan K, 2013. Regulation of cyclic AMP response element binding and hippocampal plasticity-related genes by peroxisome proliferator-activated receptor alpha. Cell Rep 4, 724–737. [PubMed: 23972989]

Roy A, Jana M, Kundu M, Corbett GT, Rangaswamy SB, Mishra RK, Luan CH, Gonzalez FJ, Pahan K, 2015. HMG-CoA Reductase Inhibitors Bind to PPARalpha to Upregulate Neurotrophin Expression in the Brain and Improve Memory in Mice. Cell Metab 22, 253–265. [PubMed: 26118928]

Roy A, Kundu M, Chakrabarti S, Patel DR, Pahan K, 2021. Oleamide, a Sleep-Inducing Supplement, Upregulates Doublecortin in Hippocampal Progenitor Cells via PPARalpha. J Alzheimers Dis 84, 1747–1762. [PubMed: 34744082]

Roy A, Kundu M, Jana M, Mishra RK, Yung Y, Luan CH, Gonzalez FJ, Pahan K, 2016. Identification and characterization of PPARalpha ligands in the hippocampus. Nat Chem Biol 12, 1075–1083. [PubMed: 27748752]

Roy A, Pahan K, 2009. Gemfibrozil, stretching arms beyond lipid lowering. Immunopharmacol Immunotoxicol 31, 339–351. [PubMed: 19694602]

Roy A, Pahan K, 2015. PPARalpha signaling in the hippocampus: crosstalk between fat and memory. J Neuroimmune Pharmacol 10, 30–34. [PubMed: 25575492]

Sabouri M, Kordi M, Shabkhiz F, Taghibeikzadehbadr P, Geramian ZS, 2020. Moderate treadmill exercise improves spatial learning and memory deficits possibly via changing PDE-5, IL-1 beta and pCREB expression. Exp Gerontol 139, 111056. [PubMed: 32791334]

Seals DF, Courtneidge SA, 2003. The ADAMs family of metalloproteases: multidomain proteins with multiple functions. Genes Dev 17, 7–30. [PubMed: 12514095]

Selkoe DJ, 1993. Physiological production of the beta-amyloid protein and the mechanism of Alzheimer's disease. Trends Neurosci 16, 403–409. [PubMed: 7504355]

Thomas R, Zimmerman SD, Yuede KM, Cirrito JR, Tai LM, Timson BF, Yuede CM, 2020. Exercise Training Results in Lower Amyloid Plaque Load and Greater Cognitive Function in an Intensity Dependent Manner in the Tg2576 Mouse Model of Alzheimer's Disease. Brain Sci 10.

Tousseyn T, Thathiah A, Jorissen E, Raemaekers T, Konietzko U, Reiss K, Maes E, Snellinx A, Serneels L, Nyabi O, Annaert W, Saftig P, Hartmann D, De Strooper B, 2009. ADAM10, the rate-limiting protease of regulated intramembrane proteolysis of Notch and other proteins, is processed by ADAMS-9, ADAMS-15, and the gamma-secretase. J Biol Chem 284, 11738–11747. [PubMed: 19213735]

Xiong JY, Li SC, Sun YX, Zhang XS, Dong ZZ, Zhong P, Sun XR, 2015. Long-term treadmill exercise improves spatial memory of male APPswe/PS1dE9 mice by regulation of BDNF expression and microglia activation. Biol Sport 32, 295–300. [PubMed: 26681831]

Yuede CM, Zimmerman SD, Dong H, Kling MJ, Bero AW, Holtzman DM, Timson BF, Csernansky JG, 2009. Effects of voluntary and forced exercise on plaque deposition, hippocampal volume,

and behavior in the Tg2576 mouse model of Alzheimer's disease. Neurobiol Dis 35, 426–432. [PubMed: 19524672]

Zhang XL, Zhao N, Xu B, Chen XH, Li TJ, 2019. Treadmill exercise inhibits amyloid-beta generation in the hippocampus of APP/PS1 transgenic mice by reducing cholesterol-mediated lipid raft formation. Neuroreport 30, 498–503. [PubMed: 30882716]

Zhao G, Liu HL, Zhang H, Tong XJ, 2015. Treadmill exercise enhances synaptic plasticity, but does not alter beta-amyloid deposition in hippocampi of aged APP/PS1 transgenic mice. Neuroscience 298, 357–366. [PubMed: 25917310]

Highlights of this study:

- Upregulation of PPARα *in vivo* in the hippocampus by treadmill exercise
- Treadmill exercise stimulates the recruitment of PPARα to *ADAM10* gene promoter *in vivo* in the hippocampus
- Failure of treadmill workout to upregulate ADAM10, reduce plaques and improve cognitive functions in 5XFAD$^{\Delta PPARα}$ mice
- Ability of treadmill exercise to upregulate ADAM10, reduce plaques and improve cognitive functions in 5XFAD$^{\Delta PPARβ}$ mice

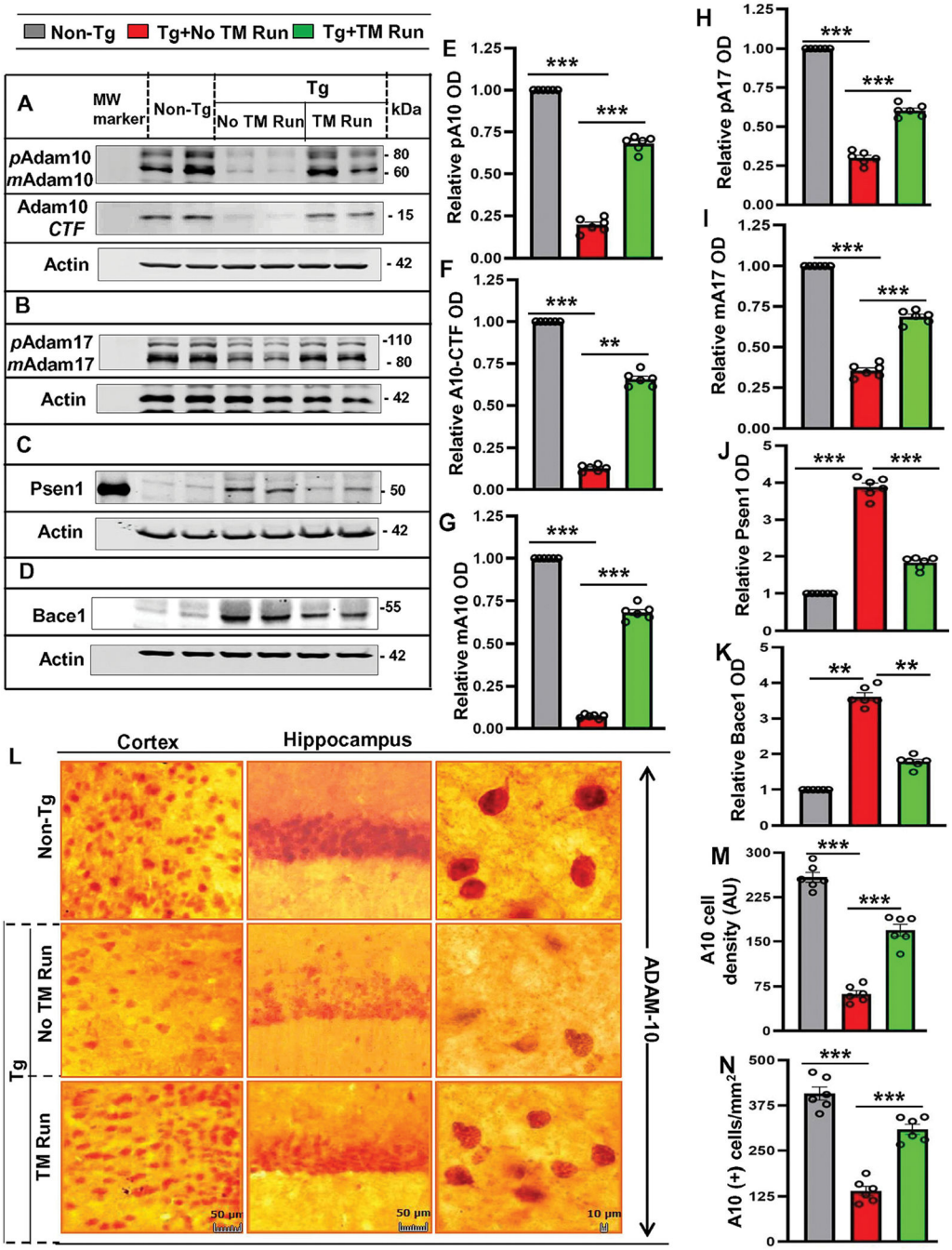

Figure 1. Treadmill exercise alters the expression of ADAM10, ADAM17, BACE1, and PSEN1 in hippocampus of Tg-mice.

Following two months of treadmill exercise, six-month-old Tg-mice (n=6/group) were sacrificed for monitoring the protein levels – *p*ADAM10, *m*ADAM10, *p*ADAM17, *m*ADAM17, Psen1, and Bace1 in hippocampus region by Western Blot using the monoclonal ADAM10 antibody. (A-D). Actin was used as the loading control. Bands were scanned and quantified using the NIH Image J software for *p*ADAM10 (E), ADAM10-*CTF* (F), *m*ADAM10 (G), *p*ADAM17 (H), *m*ADAM17 (I), PSEN1 (J) and BACE1 (K) and the results are represented as relative to non-Tg mice group. Results

are mean ± SD of six per group. *p*ADAM10 - ***$p<0.001$ (=0.0002) vs non-Tg mice and ***$p<0.001$ (=0.0027) vs Tg-mice with exercise; *m*ADAM10 - ***$p<0.001$ (=0.0034) vs non-Tg mice and ***$p<0.001$ (=0.0085) vs Tg-mice with exercise; ADAM10*CTF* - $p<0.001$ (=0.0045) vs Non-Tg mice and **$p<0.01$ (=0.0228) vs Tg-mice with exercise; *p*ADAM17 – ***$p<0.001$ ($=1.3708\times10^{-7}$) vs Non-Tg mice and ***$p<0.001$ ($=2.0546\times10^{-5}$) vs Tg-mice with exercise; *m*ADAM17 - ***$p<0.001$ (=0.000735) vs non-Tg mice and ***$p<0.001$ ($=5.6511\times10^{-5}$) vs Tg-mice with exercise; Psen1 - ***$p<0.001$ (=0.0021) vs non-Tg mice and ***$p<0.001$ (=0.0052) vs Tg-mice with exercise; Bace1 - ***$p<0.001$ (=0.0023) vs non-Tg mice and ***$p<001$ (=0.0066) vs Tg-mice with exercise. (L) Diaminobenzidine staining was performed using the polyclonal ADAM10 antibody for demonstrating the ADAM10 expression in cortex and hippocampus region of mice with treadmill exercise and compared with non-exercise group. The density and number of cells expressing ADAM10 were quantified by using the Image J (M, N) and results are mean ± SD of six per group. Statistical analyzes was conducted by using One-way ANOVA followed by Tukey's multiple comparison tests. The number of cells with ADAM10 expression - ***$p<0.001$ ($=1.6537\times10^{-24}$) vs Non-Tg mice and ***$p<0.001$ ($=2.6426\times10^{-14}$) vs Tg-mice with treadmill exercise; average density of cells expressing ADAM10 - ***$p<0.001$ ($=8.6301\times10^{-49}$) vs non-Tg mice and ***$p<0.001$ ($=2.5534\times10^{-29}$) vs Tg-mice with treadmill exercise. Abbreviations: *p*ADAM10 - proADAM10; *m*ADAM10 - matureADAM10; *p*ADAM17 - proADAM17; *m*ADAM17 - matureADAM17; ns – Non-significant.

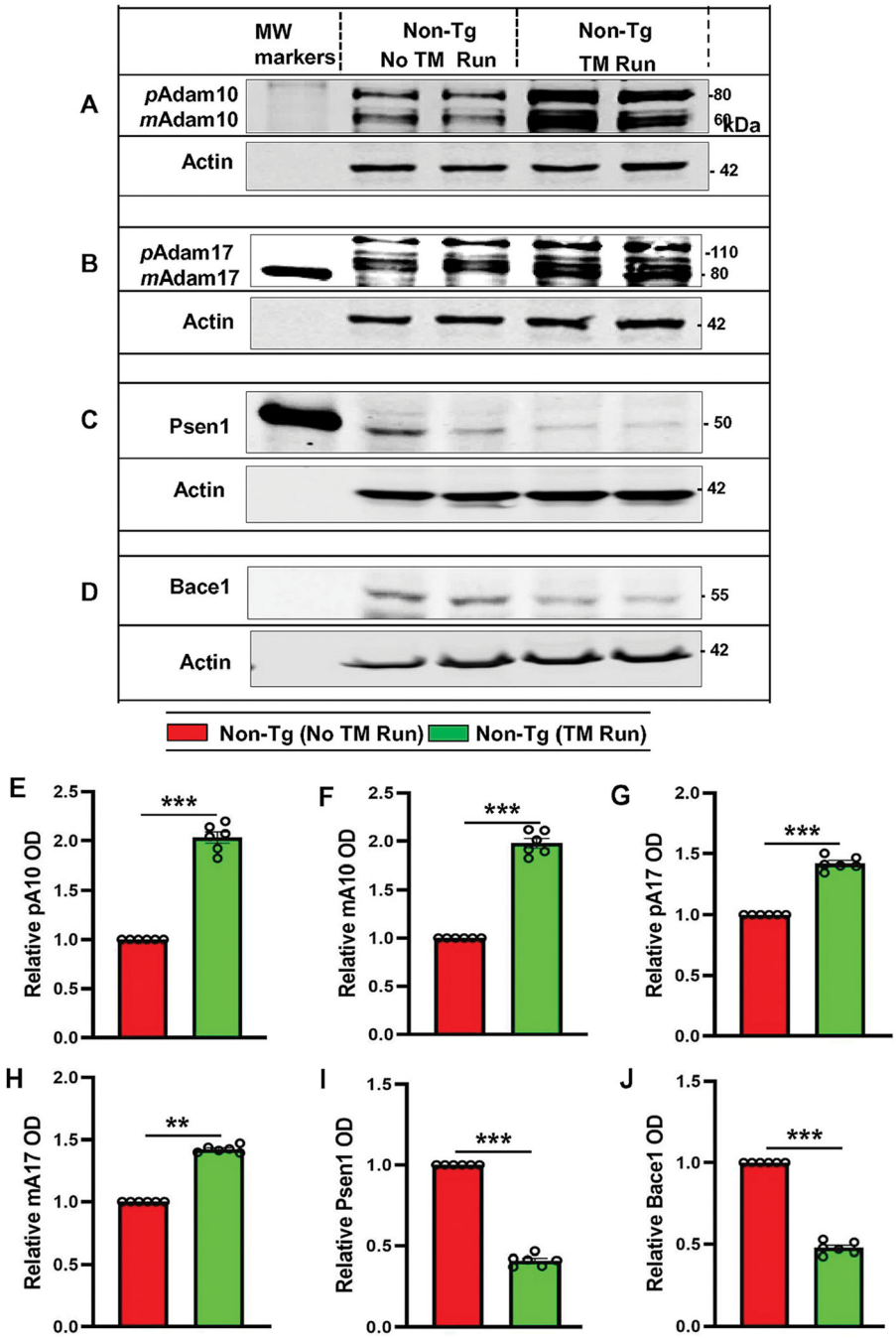

Figure 2. Treadmill exercise results in upregulation of ADAM10, ADAM17, PSEN1, and BACE1 *in vivo* in the hippocampus of non-Tg mice.

Six-month-old non-Tg mice (n=6/group) were allowed to gently run in the treadmill. After treadmill exercise, mice were sacrificed for monitoring the protein levels – *p*ADAM10, mADAM10, *p*ADAM17, *m*ADAM17, PSEN1 and BACE1 in hippocampal tissue by Western Blot (A-D). Actin was used as the loading control. Bands were scanned and quantified using the NIH Image J software for *p*ADAM10 (E), *m*ADAM10 (F), *p*ADAM17 (G), *m*ADAM17 (H), PSEN1 (I), and BACE1 (J) and the results are represented as relative to non-Tg mice. Results are mean ± SD of six per group. Statistical analysis

was conducted by using One-way ANOVA followed by Tukey's multiple comparison tests. *p*ADAM10 - ***$p<0.001$ (=0.001498) vs non-Tg mice with exercise; *m*ADAM10 - **$p<0.01$ (=0.012013) vs non-Tg mice with exercise; *p*ADAM17 – ***$p<0.001$(=0.000827) vs non-Tg mice with exercise; *m*ADAM17 - **$p<0.01$(=0.019092) vs non-Tg mice with exercise; PSEN1 - ***$p<0.001$ (=0.000397) vs non-Tg mice with exercise and BACE1 - ***$p<0.001$ (=0.009281) vs Non-Tg mice with exercise. Abbreviations: *p*ADAM10 - proADAM10; *m*ADAM10 - matureADAM10; *p*ADAM17 - proADAM17; *m*ADAM17 - matureADAM17; ns – Non-significant.

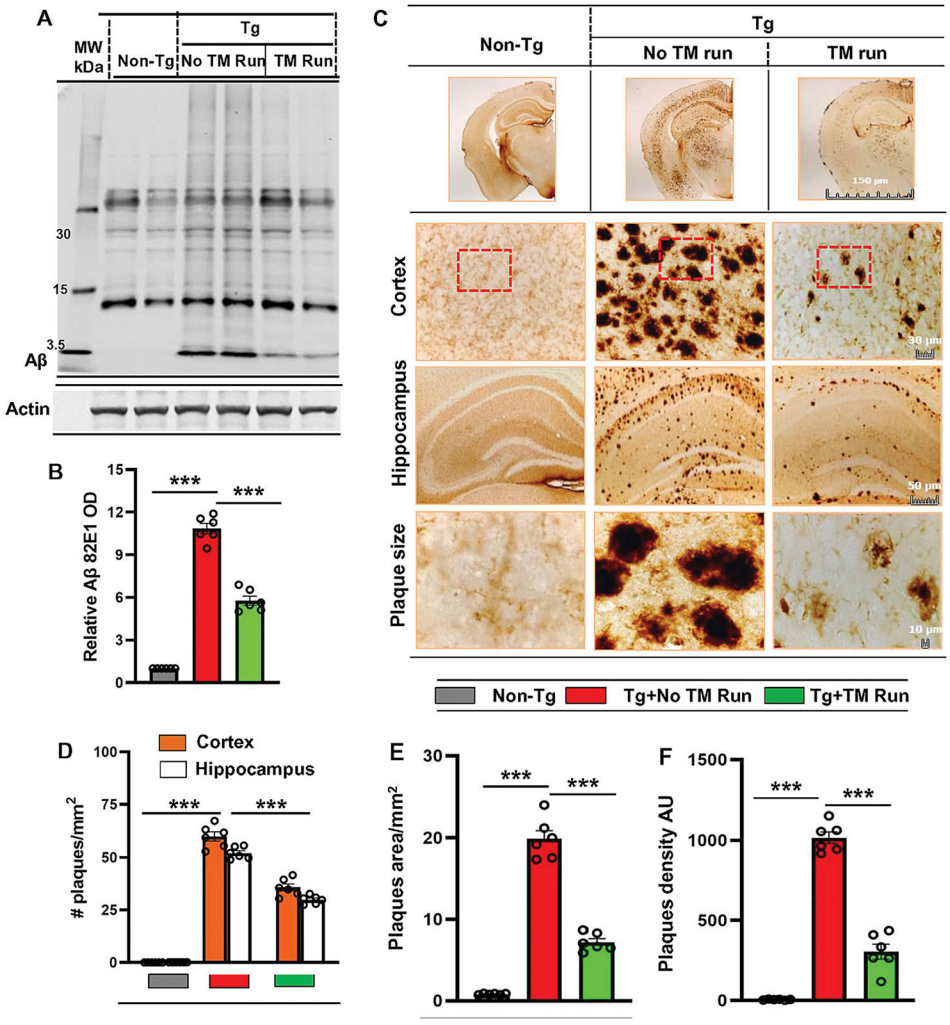

Figure 3. Treadmill exercise reduces the burden of Aβ in the hippocampal region of Tg-mice.

Six-month-old Tg-mice (n=6/group) were allowed to gently run on the treadmill. Following the treadmill exercise, Aβ levels were examined in hippocampal homogenates of different groups of mice by Western Blot using the 82E1 monoclonal antibody (A). Actin was used as the loading control. All the protein bands were scanned and densitometric analysis representing mean ± SD for Aβ levels relative to Non-Tg controls. (B) Quantification of Aβ level in protein bands indicates - ***p<0.001 (=0.0005) vs Non-Tg mice and ***p<0.001(=0.0008) vs Tg-mice with treadmill exercise. (C) Diaminobenzidine staining of hippocampal sections were performed using the monoclonal 82E1 antibody for demonstrating the Aβ pathology in cortex and hippocampus region of Tg-mice with and without treadmill exercise. The Aβ plaque pathology was characterized for number of plaques (D), average size of plaques (E) and density of plaques (F). Results are mean ± SD of six per group. All the quantification of Aβ plaques was performed using the Image J. Statistical analysis were conducted by using One-way ANOVA followed by Tukey's multiple comparison tests. The number of plaques in Cortex - ***p<0.001 (=2.8943×10^{-5}) vs non-Tg mice; ***p<0.001(=0.0005) vs Tg-mice with exercise and in hippocampus - ***p<0.001(=6.2981×10^{-5}) vs non-Tg mice; ***p<0.001(=0.0008) vs

Tg-mice with exercise. The size of plaques - ***p<0.001 (=6.1500×10^{-9}) vs non-Tg mice; ***p<0.001 (=2.44×10^{-13}) vs Tg-mice with exercise and density of plaques - ***p<0.001(=2.6173×10^{-49}) vs non-Tg mice; ***p<0.001(=9.1780×10^{-19}) vs Tg-mice with exercise. ns – Non-significant.

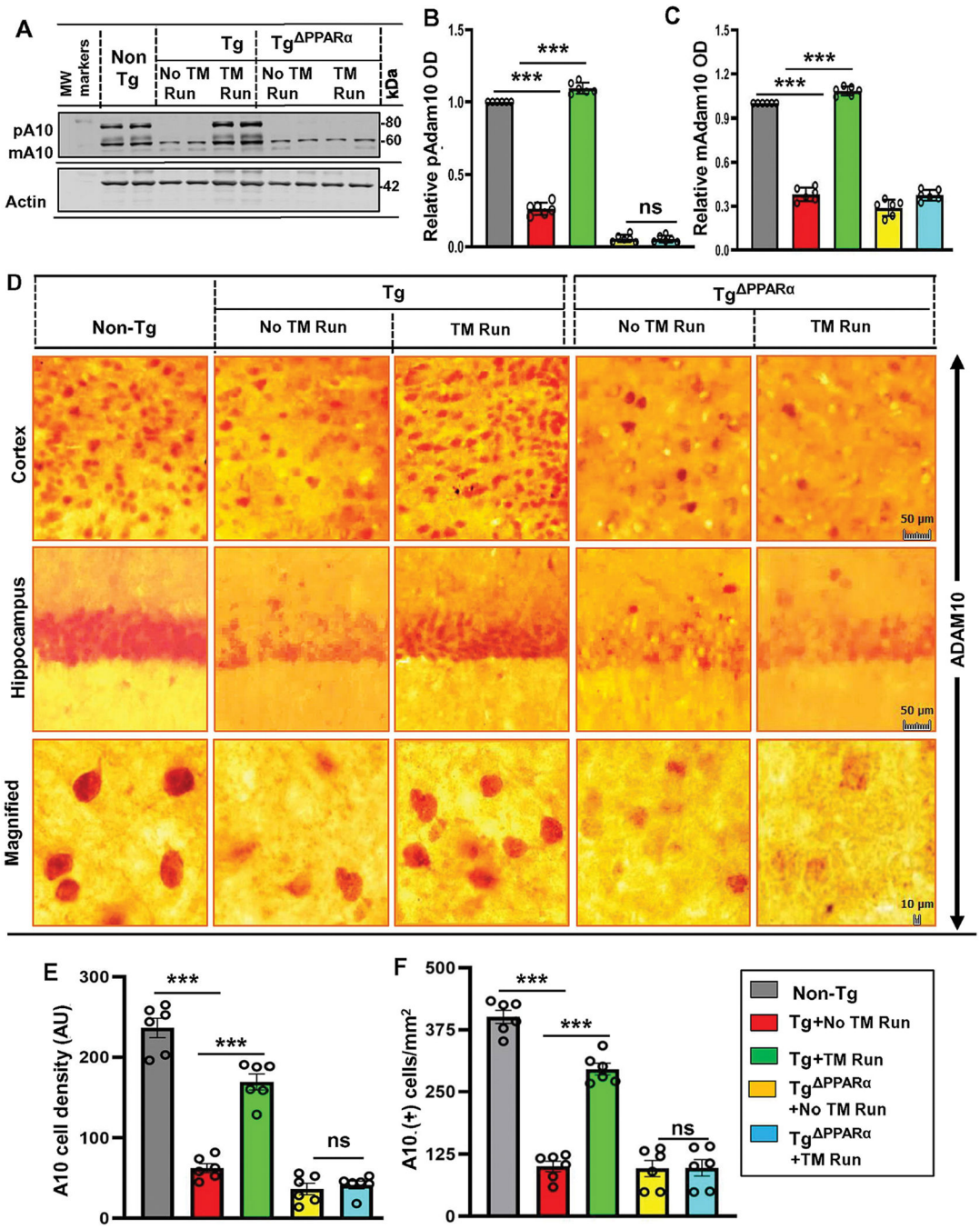

Figure 4. Treadmill exercise results in upregulation of ADAM10 via the PPARα pathway.

Six-month-old Tg-mice and $Tg^{\Delta PPAR\alpha}$ mice (n=6/group) were initially allowed to perform running exercise on the rotating treadmill. After treadmill exercise, mice were sacrificed for monitoring the level of *p*ADAM10 and *m*ADAM10 in hippocampal homogenates by Western blot (A). Actin was used as the loading control. Bands were scanned and densitometric analysis for *p*ADAM10 and *m*ADAM10 levels relative to non-Tg controls were performed using the NIH Image J Software. (B, C) Quantification of relative ADAM10 level in protein bands are mean ± SD of six per group indicates - for *p*ADAM10 – $p<0.001$

(=0.0021) vs non-Tg mice; $p<0.001$ (=0.0033) vs Tg-mice with exercise; ns (=0.8117) vs $Tg^{\Delta PPAR\alpha}$ mice without exercise and for *p*ADAM10 - $p<0.001$ (=0.0002) vs non-Tg mice; $p<0.001$ (=0.0001) vs Tg-mice with exercise; ns (=0.0211) vs $Tg^{\Delta PPAR\alpha}$ mice without exercise. (D) Diaminobenzidine staining of hippocampal sections were performed using the monoclonal ADAM10 antibody for demonstrating the ADAM10+ cells in cortex and hippocampus region of mice in Tg-mice and $Tg^{\Delta PPAR\alpha}$ mice with and without treadmill exercise. Results are mean ± SD of six per group. All the quantification of Aβ plaques was performed using the Image J. Statistical analysis were conducted by using One-way ANOVA followed by Tukey's multiple comparison tests. (E) The A10+ cell density - ***$p<0.001$ ($=8.6301\times10^{-49}$) vs non-Tg mice; ***$p<0.001$ ($=2.5534\times10^{-29}$) vs Tg-mice; ns (=0.1274) vs $Tg^{\Delta PPAR\alpha}$ mice with exercise and (F) the number of A10+ cells - ***$p<0.001$ ($=1.6537\times10^{-24}$) vs non-Tg mice; ***$p<0.001$ ($=2.6426\times10^{-14}$) vs Tg-mice with exercise; ns (=0.8463) vs $Tg^{\Delta PPAR\alpha}$ mice with exercise. (*p*ADAM10 – proADAM10; *m*ADAM10 - mature ADAM10 and. ns – Non-significant).

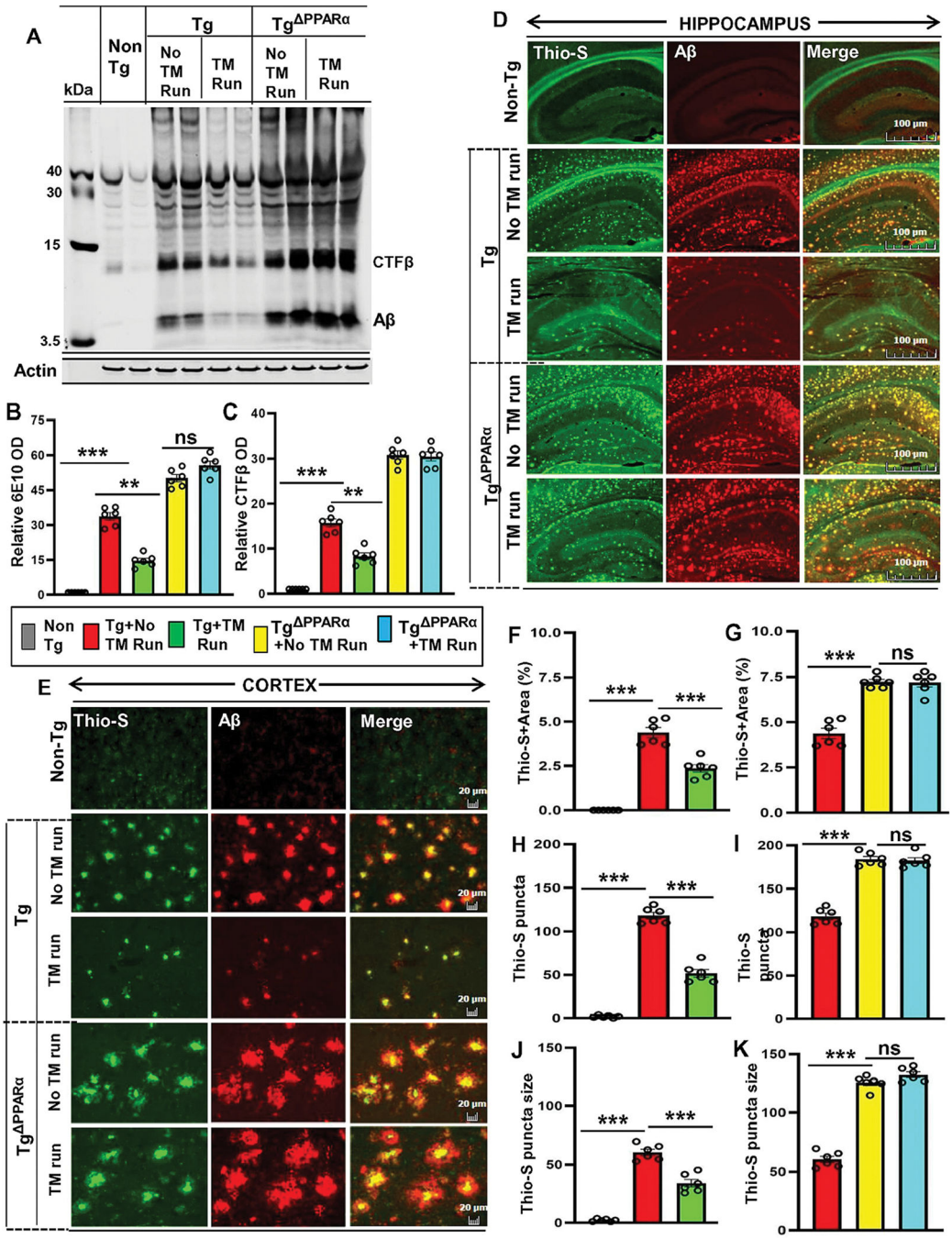

Figure 5. Treadmill exercise reduces the burden of Aβ in Tg-mice via the PPARα pathway.

Aβ level was analyzed in six-month-old Tg-mice and $Tg^{\Delta PPAR\alpha}$ mice after treadmill exercise and compared with non-exercise group of mice. Using the 6E10 monoclonal antibody, the level of Aβ proteins were examined in the hippocampal homogenates of mice by the Western blot (A). Actin was used as the loading control. All the protein bands were scanned and densitometric analysis representing mean ± SD for Aβ levels relative to non-Tg controls. Quantification of relative Aβ level (B) and CTF-β level (C) in protein bands indicates - ***p<0.001(=0.0016) vs non-Tg mice; ***p<0.001 (=0.0012) vs Tg-mice

with exercise; ns (=0.4829) vs $Tg^{\Delta PPAR\alpha}$ mice with exercise and ***p<0.001(=0.0018) vs non-Tg mice; ***p<0.001 (=0.0025) vs Tg-mice with exercise; ns (=0.7484) vs $Tg^{\Delta PPAR\alpha}$ mice with exercise. (D, E) Hippocampal sections were double-labeled using the Thio-S and Aβ 6E10 antibody for demonstrating the Aβ pathology in cortex and hippocampus region of Tg-mice and $Tg^{\Delta PPAR\alpha}$ mice with and without treadmill exercise. Results are mean ± SD of six per group. All the quantification of Aβ plaques was performed using the Image J. Statistical analysis were conducted by using One-way ANOVA followed by Tukey's multiple comparison tests. Thio-S positive plaques in hippocampus and cortex were further characterized for (F, G) the total area fraction (Thio-S area as a percentage of total hippocampal area) - ***p<0.001(=1.8100×10^{-18}) vs non-Tg mice and ***p<0.001(=8.9453×10^{-9}) vs Tg-mice with exercise; ns (=0.1552) vs $Tg^{\Delta PPAR\alpha}$ mice with exercise; (H, I) the plaque count - ***p<0.001 (=1.9361×10^{-26}) vs non-Tg mice and ***p<0.001 (=2.0106×10^{-11}) vs Tg-mice with exercise; ns (=0.3492) vs $Tg^{\Delta PPAR\alpha}$ mice with exercise; (J, K) the average plaque size – p***0.001 (=4.6257×10^{-14}) vs non-Tg mice and ***p<0.001(=9.9493×10^{-7}) vs Tg-mice with exercise; ns (=0.5694) vs $Tg^{\Delta PPAR\alpha}$ mice with exercise. ns – Non-significant.

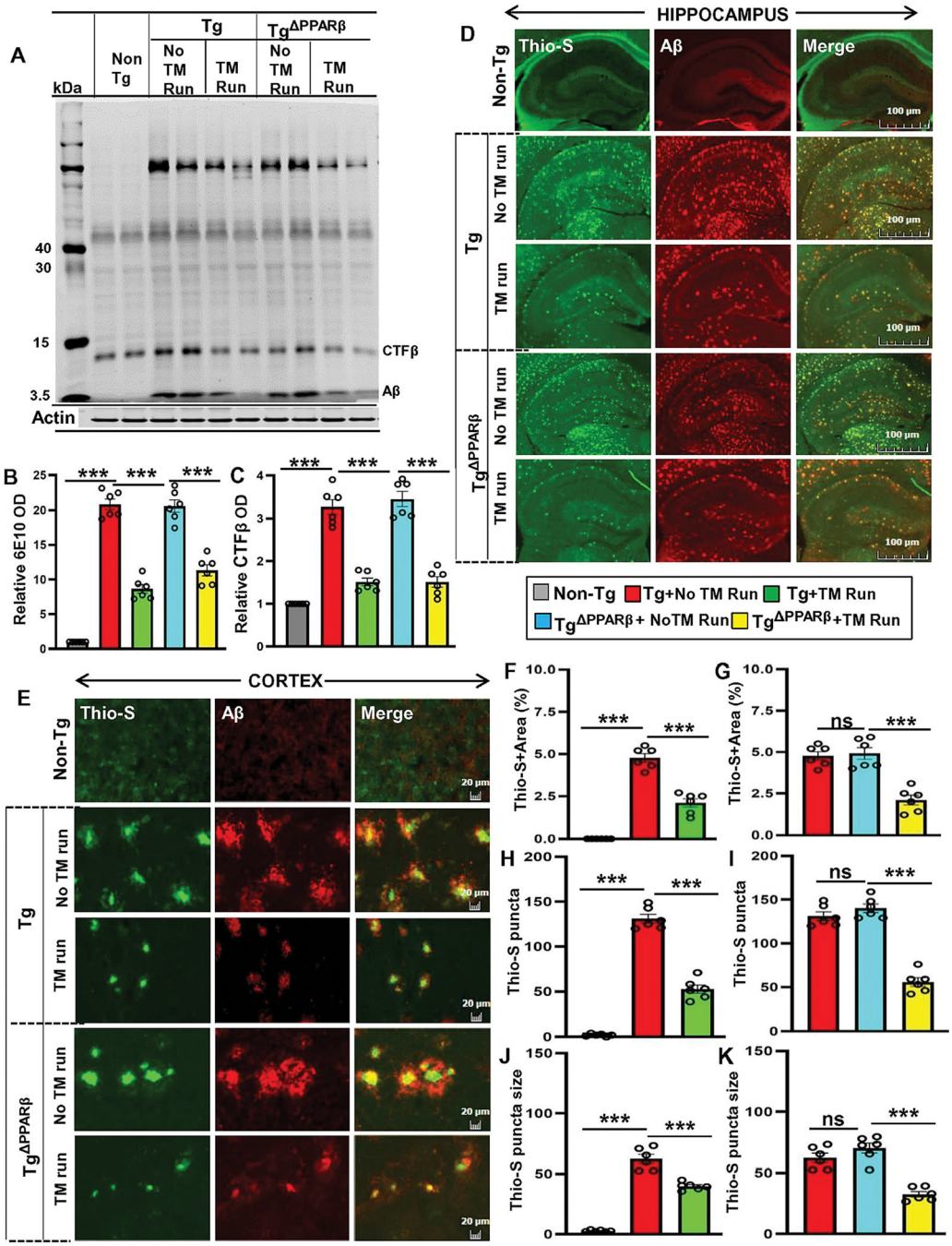

Figure 6. Treadmill exercise reduces the burden of Aβ in $Tg^{\Delta PPAR\beta}$ mice.

Following the treadmill exercise, the level of Aβ proteins were examined in six-month old Tg-mice and $Tg^{\Delta PPAR\beta}$ mice (n=6/group) and compared with non-exercise groups of mice. Using the 6E10 monoclonal antibody, the Aβ levels was analyzed in the hippocampal homogenates in Tg-mice and $Tg^{\Delta PPAR\beta}$ mice by the Western blot (A). Actin was used as the loading control. All the protein bands were scanned and densitometric analysis representing mean ± SD for Aβ levels relative to non-Tg controls. Quantification of protein bands for (B) relative Aβ level indicates - ***p<0.001(=0.0051) vs non-Tg mice; ***p<0.001 (=0.0016)

vs Tg-mice with exercise; ***p<0.01 (=0.0115) vs $Tg^{\Delta PPAR\beta}$ mice with exercise and (C) CTF-β level - ***p<0.001 (=9.4200 ×10^{-5}) vs non-Tg mice; ***p<0.001(=2.2000×10^{-5}) vs Tg-mice with exercise; ***p<0.001 (=0.0002) vs $Tg^{\Delta PPAR\beta}$ mice with exercise. (D, E) Hippocampal sections were double labeled using Thio-S and Aβ 6E10 antibody for demonstrating the Aβ pathology in cortex and hippocampus region of Tg-mice and $Tg^{\Delta PPAR\beta}$ mice with and without treadmill exercise. Results are mean ± SD of six per group. All the quantification of Aβ plaques was performed using the Image J. Statistical analysis were conducted by using One-way ANOVA followed by Tukey's multiple comparison tests. Thio-S positive plaque in hippocampus and cortex were further characterized for (F, G) the total area fraction (Thio-S area as a percentage of total hippocampal area) - ***p<0.001(=5.9402×10^{-9}) vs non-Tg mice and ***p<0.001 (=8.8417×10^{-6}) vs Tg-mice with exercise; ***p<0.001 (=0.0007) vs $Tg^{\Delta PPAR\beta}$ mice with exercise; (H, I) the average plaque size – p***0.001 (=9.5979×10^{-11}) vs non-Tg mice and ***p<0.001 (=3.9553×10^{-5}) vs Tg-mice with exercise; ***p<0.001 (=6.3974×10^{-5}) vs $Tg^{\Delta PPAR\beta}$ mice with exercise; (J, K) the plaque count - ***p<0.001 (=1.1730×10^{-11}) vs non-Tg mice and ***p<0.001 (=8.0403×10^{-11}) vs Tg-mice with exercise; ***p<0.001 (=4.0153×10^{-8}) vs $Tg^{\Delta PPAR\beta}$ mice with exercise. ns – Non-significant.

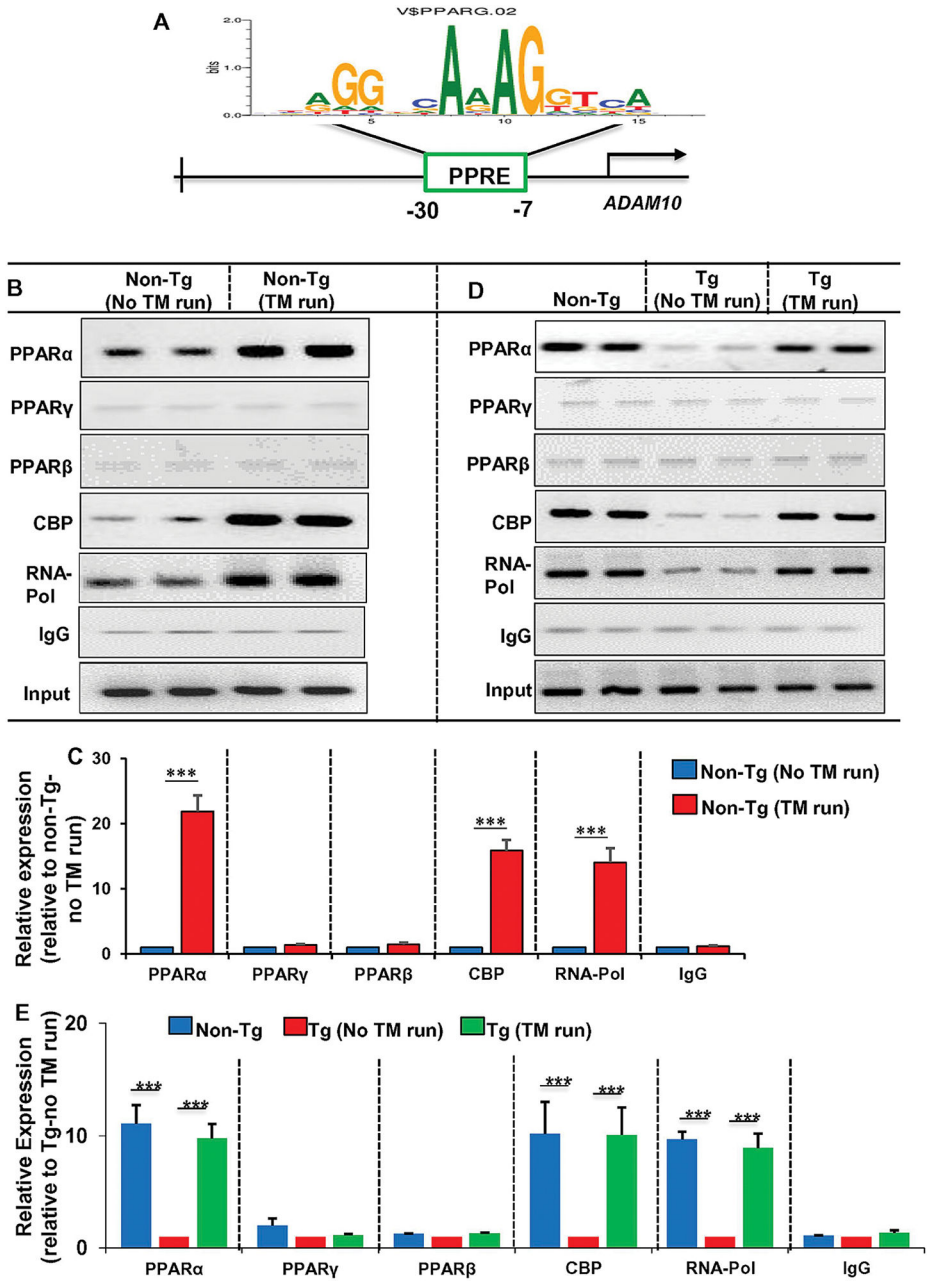

Figure 7. Treadmill exercise stimulates the recruitment of PPARα to the *ADAM10* gene promoter *in vivo* in the hippocampus of Tg mice.

The schematic diagram shows the presence of PPRE in the *ADAM10* promoter very close (−7 bp to −30 bp) to the transcription start site (A). Genomic DNA was isolated from hippocampal tissues of normal as well as treadmill-exercised non-Tg (B & C) and Tg (D & E) mice and binding of PPARα, PPARβ, PPARγ, CBP, and RNA polymerase to the PPRE site was analyzed by chromatin immunoprecipitation (ChIP) followed by semi-quantitative (B & D) and real-time PCR (C & E) quantification of the PPRE-containing 205 bp fragment. Results are mean ± SEM of four mice per group. ***$p < 0.001$.